Sussex Research Online

Human BRCA1-BARD1 ubiquitin ligase activity counters chromatin barriers to DNA resection

Article (Accepted Version)

Densham, Ruth M, Garvin, Alexander J, Stone, Helen R, Strachan, Joanna, Baldock, Robert A, Daza-Martin, Manuel, Fletcher, Alice, Blair-Reed, Sarah, Beesley, James, Johal, Balraj, Pearl, Laurence H, Neely, Robert, Keep, Nicholas H, Watts, Felicity Z and Morris, Joanna R (2016) Human BRCA1-BARD1 ubiquitin ligase activity counters chromatin barriers to DNA resection. Nature Structural and Molecular Biology, 23 (7). pp. 647-655. ISSN 1545-9993

This version is available from Sussex Research Online: http://sro.sussex.ac.uk/id/eprint/60891/

This document is made available in accordance with publisher policies and may differ from the published version or from the version of record. If you wish to cite this item you are advised to consult the publisher's version. Please see the URL above for details on accessing the published version.

Copyright and reuse:
Sussex Research Online is a digital repository of the research output of the University.

Copyright and all moral rights to the version of the paper presented here belong to the individual author(s) and/or other copyright owners. To the extent reasonable and practicable, the material made available in SRO has been checked for eligibility before being made available.

Copies of full text items generally can be reproduced, displayed or performed and given to third parties in any format or medium for personal research or study, educational, or not-for-profit purposes without prior permission or charge, provided that the authors, title and full bibliographic details are credited, a hyperlink and/or URL is given for the original metadata page and the content is not changed in any way.

http://sro.sussex.ac.uk

Human BRCA1-BARD1 Ubiquitin ligase activity counters chromatin barriers to DNA resection.

Ruth M Densham[1], Alexander J. Garvin[1], Helen R. Stone[1] , Joanna Strachan[1, 5] , Robert A Baldock[2], Manuel Daza-Martin[1], Alice Fletcher[1], Sarah Blair-Reid[1], James Beesley[1], Balraj Johal[1], Laurence H. Pearl[2], Robert Neely[3], Nicholas H. Keep[4], Felicity Z Watts[2] and Joanna R. Morris[1]

1. Birmingham Centre for Genome Biology and Institute of Cancer and Genomic Sciences, University of Birmingham, Birmingham, United Kingdom.
2. Genome Damage and Stability Centre, School of Life Sciences, University of Sussex, Brighton, United Kingdom.
3. School of Chemistry, University of Birmingham, Birmingham, United Kingdom.
4. Department of Biological Sciences, Institute for Structural and Molecular Biology, Birkbeck, University of London, United Kingdom.
5. Present address: Institute of Cell Biology, University of Edinburgh, Edinburgh, United Kingdom.

Corresponding author: Jo Morris j.morris.3@bham.ac.uk

Abstract

The opposing activities of 53BP1 and BRCA1 influence pathway choice of DNA double-strand break repair. How BRCA1 counters the inhibitory effect of 53BP1 on DNA resection and homologous recombination is unknown. Here we identify the site of BRCA1-BARD1 required for priming ubiquitin transfer from E2~ubiquitin. We demonstrate that BRCA1-BARD1's ubiquitin ligase activity is required for repositioning 53BP1 on damaged chromatin. We confirm H2A ubiquitylation by BRCA1-BARD1 and show that an H2A-ubiquitin fusion protein promotes DNA resection and repair in BARD1 deficient cells. We show BRCA1-BARD1 function in homologous recombination requires the chromatin remodeler SMARCAD1. SMARCAD1 binding to H2A-ubiquitin, optimal localization to sites of damage and activity in DNA repair requires its ubiquitin-binding CUE domains. SMARCAD1 is required for 53BP1 repositioning and the need for SMARCAD1 in Olaparib or camptothecin resistance is alleviated by 53BP1 loss. Thus BRCA1-BARD1 ligase activity and subsequent SMARCAD1-dependent chromatin remodeling are critical regulators of DNA repair.

Introduction.

Inheritance of a mutation in the breast cancer susceptibility gene 1 (*BRCA1*) confers a high risk of breast and ovarian cancer, and tumours in *BRCA1* gene mutation carriers are characterized by excessive genome instability. The BRCA1 protein is implicated in several aspects of genome stability: including check-point promotion, DNA cross-link repair, replication fork stability and DNA double-strand break (DSB) repair[1-3]. In DSB repair it is most prominently associated with homologous recombination (HR) where it promotes the essential step of DNA resection by opposing the block on resection contributed by the p53 binding protein 53BP1 and its effector proteins (reviewed in [3,4]). In the absence of BRCA1, DSBs are repaired by toxic non-homologous end joining (NHEJ)[5]. BRCA1 associates with the resection protein CtIP to relieve the 53BP1 block[6], but how BRCA1 contributes is not known.

In familial breast and ovarian cancer patients, pathogenic and unclassified substitution variants in the *BRCA1* gene are found across the region encoding the first hundred amino acids. This part of BRCA1 contacts its heterodimeric binding partner, the BRCA1-associated RING domain protein ,BARD1, and E2 Ubiquitin (Ub) conjugating enzymes, allowing BRCA1-BARD1 to function as an E3 Ub ligase in the transfer of Ub from E2 conjugating enzymes to target proteins[7]. Several targets have been proposed and recently BRCA1-mediated ubiquitination of histone 2A (H2A) has been mapped[8]. However a role, if any, played by the BRCA1 E3 Ub ligase activity in DNA repair has been controversial[9-11]. Evidence from *Brca1* deficient mice has suggested H2A ubiquitination regulates global heterochromatin integrity, and through transcriptional repression of satellite RNA is responsible for multiple disparate cellular functions of Brca1, including the promotion of genomic integrity[9]. How increased satellite RNA impacts HR repair is not clear and the phenomenon of increased satellite RNA expression has not been universally observed in *Brca1* deficient models [12]. Indeed other models of Brca1 dysfunction have suggested a restricted role, or no role, for its biochemical function in DNA repair[10,11].

Here we set out to investigate the role of the BRCA1-BARD1 Ub ligase activity in the DNA damage response in human cells. Our data suggest a model in which chromatin modification by BRCA1-BARD1 E3 Ub ligase activity repositions 53BP1 and drives completion of resection through promoting the activity of the SWI/SNF-Related, Matrix-Associated Actin-Dependent Regulator of Chromatin, SMARCAD1.

Results

A charged residue required in Type 1 RING:RING E3s.

Ub priming structures that promote the transfer of the donor Ub from a Ub-loaded E2 conjugating enzyme have been identified in RING finger protein 4, RNF4, and Casitas B-lineage Lymphoma, C-CBL, E3 Ub ligases[13,14]. However no surfaces analogous to these have yet been found in E3 Ub ligases characterized by helical interactions between protomers, known as Type I [15]. These include the human homologue of yeast radiation mutant 18 (RAD18), the polycomb repressor complex ligase RING1A or RING1B complexes and BRCA1-BARD1. Nevertheless minimal BRCA1-BARD1 N-terminal fragments exhibit base-level Ub ligase activity[16,17] indicating that the elements necessary for Ub transfer are present within the polypeptides.

To identify a possible Ub-binding interface we overlaid the RNF4-RNF4-Ub~E2 structure (PDB: 4AP4[13]) onto N-terminal BRCA1-BARD1 (PDB: 1JM7[18]). In the superposition BARD1 residues 91-99 are in a similar location to the RNF4 residue, Y193, which engages Ub[13]. A mutational scan across the BARD1 region revealed that a heterodimer bearing a substitution at R99 exhibited reduced activity (Supplemental Fig. 1A&B). Substitution of R99 to a lysine was tolerated but the activity of the heterodimer with glutamic acid (R99E) was severely impaired with all Ub conjugating enzymes of the Ub-Conjugating Enzyme 2D (UBE2D) family (Fig 1A, Supplemental Fig. 1C-E). Substitutions at R99 did not affect BARD1 interaction with BRCA1 (Fig 1B) but the R99E mutant heterodimer showed a weaker interaction with conjugation-proficient E2 (Supplemental Fig. 1F).

In the superimposition R99-BARD1 is predicted to be close to the D32 side chain of Ub (Supplemental Fig. 1G). To test whether R99-BARD1 contacts Ub, we made a D32R mutation in Ub. This mutant was processed slightly less well than Wild Type (WT) Ub by the BRCA1-BARD1 heterodimer, but the weak catalytic activity of the R99E-BARD1 mutant heterodimer was substantially improved with D32R-Ub (Fig 1C), suggesting contact with Ub contributes to activity. Transfer reactions of Ub from UBE2D1 or UBE2D3 E2 enzymes to free lysine revealed reduced discharge rates with the R99E heterodimer compared to WT proteins (Fig 1D, Supplemental Fig 1H). Thus R99-BARD1 promotes heterodimer interaction with the Ub~E2 thioester conjugate through Ub and is required to promote the discharge of Ub from the E2 contacting BRCA1.

We noted that other Type 1 RING E3 ligases carry positively charged residues (R or K) at positions analogous to R99-BARD1 (Fig 2A & Supplemental Fig 2A). For example in the heterodimeric protein formed of B cell-specific Moloney murine leukemia virus integration site 1, BMI1 (also known as polycomb group RING finger protein 4 (PCGF4)) with RING1B, BMI1-RING1B, the 'inactive' partner, BMI1, has an equivalent lysine, K73, while the protomer contacting the E2, RING1B, lacks a similarly located charged residue (as does BRCA1). We mutated K73E in BMI1 and R76A in RAD18. While WT RAD18 induced PCNA mono-ubiquitination on ectopic expression and also potentiated PCNA mono-ubiquitination following UV exposure, the R76A mutant failed to do so (Fig. 2B). Similarly the K73E-BMI1-RING1B heterodimer lacked the ability to catalyze mono-ubiquitination of H2A in nucleosomes *in vitro* (Fig. 2C, see Supplemental Fig. 2B for co-purification). In cells ectopic expression of K73E-BMI1 but not WT protein inhibited DSB Ub signaling and WT-BMI1 but not K73E-BMI1 was able to rescue repair of a gene conversion substrate in cells depleted of endogenous BMI1 (Supplemental Fig. 2C-E). These data are consistent with the effect of inhibiting RING1A and RING1B[19]. We suggest that a charged interface between Type I dimeric RING E3 ligases and the donor Ub activates the E2~Ub thioester. In the two heterodimeric complexes this key interface is provided by protomers previously described as simply scaffold proteins, BARD1 and BMI1.

Ligase activity is required for a subset of BRCA1 responses.

To address possible roles of the BRCA1-BARD1 Ub ligase activity we depleted HeLa cells of endogenous BARD1 and expressed siRNA resistant full length WT BARD1 cDNA or mutant forms bearing BARD1 amino acid substitutions R99E or L44R (illustrated in Fig. 3A). L44R

introduces a large hydrophilic residue in the hydrophobic helical face of BARD1 preventing interaction with BRCA1 [20]. Complementation of cells with L44R-BARD1 failed to support heterodimer formation, heterodimer stability, or promote endogenous BRCA1 localization to irradiation-induced foci (IRIF) (Supplemental Fig. 3A-C). In contrast R99E-BARD1 retained dimerization with BRCA1, promoted both BRCA1 stability and localization to IRIF (Supplemental Fig. 3A-C). Neither R99E-BARD1, nor L44R-BARD1 purified complexes exhibited Ub ligase activity (Supplemental Fig. 3D). Thus L44R-BARD1 is both heterodimer and ligase disruptive in cells, whereas the R99E-BARD1 variant is ligase defective but promotes heterodimer formation.

To differentiate potential roles for ligase activity from those of the heterodimer in DNA repair we compared survival of cells depleted for endogenous BARD1 and complemented with the separation of function variants in response to various DNA damaging agents. BARD1 depletion or complementation with L44R-BARD1 resulted in sensitivity to each DNA damaging agent tested and complementation with the WT-BARD1 protein restored resistance (Fig. 3B). Strikingly R99E-BARD1 complemented cells exhibited resistance to some agents but not to others. They were resistant to replication fork stalling and slowing agents, hydroxyurea (HU) and aphidicolin, and to the intra-strand-cross-linking (ICL) agent, cisplatin, but sensitive to camptothecin (topoisomerase-I poison), etoposide (topoisomerase-II poison), Olaparib (AZD-2281, PARP inhibitor) and irradiation (Fig. 3B). These data prompted us to revisit the I26A substitution of BRCA1 that disrupts interaction with E2 conjugating enzymes ([7]and also shown in Supplemental Fig. 3E). Cells depleted for endogenous BRCA1 and complemented with I26A-BRCA1 were also sensitive to Olaparib (Fig. 3C), supporting the notion that the BRCA1-BARD1 Ub ligase activity supports Olaparib resistance.

Ligase activity promotes 53BP1 repositioning and resection.

The sensitivities of ligase defective cells suggest a role in the promotion of HR, a process begun by resection of DNA ends. To interrogate the HR pathway, we first examined the ssDNA binding protein Replication protein A (RPA), which forms foci after irradiation and is indicative of resection. Cells complemented with R99E-BARD1 or L44R-BARD1 exhibited reduced numbers, size and intensity of RPA foci and also had reduced foci of the human homologue of yeast radiation mutant 51, RAD51, compared to WT-BARD1 complemented cells (Fig 4A, Supplemental Figure 4A). These data suggest ligase activity relates to the role of BRCA1 in promoting DNA resection prior to formation of the RAD51 nucleofilament in HR.

53BP1 and its effector proteins act to block DNA resection in the absence of BRCA1[4]. As anticipated, depletion of 53BP1 alleviated the requirement for BRCA1-BARD1 Ub ligase activity in Olaparib and Camptothecin resistance, increased RAD51 and RPA foci after IR and improved repair of an integrated HR substrate in a manner that was dependent on the 'CtBP-Interacting Protein' and nuclease, CtIP (Fig 4B, Supplemental Fig. 4B-F). Depletion of the 53BP1 effector proteins, human REV7 (also known as MAD2 mitotic arrest deficient-like 2, MAD2L2)[21,22]or Artemis [23], similarly improved survival of R99E-BARD1 complemented cells after IR, Olaparib or camptothecin to differing degrees depending on the agent (Supplemental Fig. 5A-C).

These data reveal for the first time that the Ub ligase activity of BRCA1-BARD1 contributes to the function of BRCA1 in DNA resection, and consistent with the described relationship between BRCA1 and 53BP1 it can be by-passed by loss of 53BP1 or its effector proteins. In

contrast, the resistance of BRCA1 depleted cells to HU was not restored by 53BP1 depletion (Fig. 4C) consistent with the notion that the Ub ligase-independent function(s) of BRCA1 do not interact with 53BP1.

The recruitment of BRCA1 into the core of IRIF is associated with eviction of 53BP1 to the periphery of the foci co-incident with RPA recruitment to the core [24,25]. We measured the distribution of 53BP1 in foci associated with BRCA1 in BARD1 depleted cells complemented with WT or R99E-BARD1 protein. While the distribution of BRCA1 within IRIF in these cells was similar, in R99E-BARD1 complemented cells eviction of 53BP1 to the periphery was markedly reduced compared to WT-BARD1 complemented cells (Fig. 4D). Thus the ligase activity plays a role in 53BP1 repositioning at IRIF.

Ligase activity in resection is needed after HR-commitment.

Resection consists of an initiation step, requiring the nuclease CtIP and Meiotic Recombination 11 Homolog A (MRE11) endonuclease activity, and an elongation stage which requires MRE11 exonuclease activity and then extension by Exonuclease 1 (EXO1) or Bloom Syndrome RecQ helicase, BLM and DNA replication helicase/nuclease 2 (DNA2) (reviewed in [26]). To assess where in resection the BRCA1-BARD1 Ub ligase activity is required we incubated cells with Bromodeoxyuridin (BrdU) and then measured track-lengths of exposed BrdU epitope, indicative of ssDNA as a measure of resected DNA after Olaparib exposure (after Cruz-Garcia *et al*., 2014 [27]). R99E-BARD1 complemented cells or BARD1 depleted cells showed shorter resection lengths. These were similar to cells exposed to MRE11 exonuclease inhibitor MIRIN but not as severely truncated as those in cells exposed to the MRE11 endonuclease inhibitor, PFM01 (Fig. 5A). These data suggest that some resection occurs in BRCA1-BARD1 ligase defective cells subsequent to the requirement for MRE11 endonuclease activity.

Incomplete resection after commitment results in IR sensitivity which can be largely rescued by inhibiting resection initiation by depleting CtIP, since loss of CtIP prevents HR commitment but allows repair by NHEJ[28]. We found that depletion of CtIP improved repair of a NHEJ substrate, but not an HR substrate in BARD1 depleted cells (Fig 5B -D) and restored the majority of the resistance of R99E-BARD1 complemented or BARD1 depleted cells to IR (Fig 5E). These data functionally confirm that the requirement for BRCA1 ligase activity occurs after HR commitment. They also suggest that in BRCA1-BARD1 deficient cells, or in cells lacking its Ub ligase function, most sensitivity to IR is a consequence of incomplete resection and poor NHEJ, and a smaller proportion due to HR deficiency.

An H2A-Ub fusion promotes DNA resection.

We next assessed possible targets of BRCA1-BARD1 ubiquitination including 53BP1, its effector proteins and histones. We irradiated cells transfected with constructs expressing His-Myc-tagged Ub and BARD1 and purified covalently bound Ub-conjugates in highly denaturing conditions. 53BP1 and H2A were enriched in WT-BARD1 expressing cells but reduced in cells expressing R99E-BARD1 mutants (Fig. 6A), suggesting that BRCA1-BARD1 E3 ligase activity results in ubiquitination of these two proteins. H2A-modification can be seen in the R99E-BARD1 lane on high exposure, indicating an additional, expected, BRCA1-BARD1 independent modification.

H2A has previously been identified as a BRCA1-BARD1 Ub ligase target [8,9,17], modified at C-

terminal lysines K125, K127 and K129[8]. We attempted to replace a proportion of endogenous H2A (which is expressed from several genes) with mutant histone by generating stable cell lines bearing H2A-K125, 127 & 129 R. However, expression of the H2A mutants had no impact on Olaparib sensitivity, suggesting either modification elsewhere is important for resistance or insufficient mutant histone incorporation was achieved (Supplemental Fig. 6A & B).

As an alternative approach we generated a H2A mutant-ubiquitin fusion protein, and addressed whether this can complement cells depleted of BARD1. In the H2A fusion lysines 13, 15, 118, 119, 125, 127 & 129 were mutated to arginines in order to interrogate the function of the fused Ub in the absence of endogenous ubiquitination events and the Ub itself was mutated at all 7 lysines to prevent chain formation. Both exogenous H2A and H2A-Ub fusion were incorporated into chromatin (Fig. 6B). In agreement with the finding that expression of a similar fusion improved repair of a gene conversion substrate in BRCA1-deficent cells[9], we confirmed that expression of the H2A-Ub protein promoted repair of a gene conversion substrate in BARD1 depleted cells (Supplemental Fig. 6C & D). To address whether H2A-Ub has the ability to restore physiological HR we examined the formation of RAD51 foci in BARD1 depleted cells. In a dose-response experiment we found that H2A-Ub levels correlated with RAD51 foci restoration, suggesting greater incorporation of the protein into chromatin resulted in greater rescue (Fig. 6C, Supplemental Fig. 6E). Moreover, neither the degree of gene conversion nor number of RAD51 foci in H2A-Ub expressing cells was further increased when 53BP1 was depleted (Supplemental Fig. 6D & F) indicating that H2A-Ub expression and the removal of 53BP1 have similar impacts. Consistent with an ability to complement the lack of BRCA1-BARD1 ligase activity in HR, expression of H2A-Ub promoted the survival of BARD1 depleted cells to Olaparib and Camptothecin but did not restore their resistance to HU (Supplemental Fig 6G-I), correlating with the requirement for BRCA1-BARD1 ligase activity. As anticipated both the drug resistance and restoration of RAD51 conferred by H2A-Ub required CtIP (Supplemental Fig 6J & K). Together these data provide strong evidence that the H2A-Ub fusion can restore physiological resection and HR in BARD1 depleted cells.

We then examined the specifics of the H2A-Ub fusion in more detail. We tested an alternative globular protein, blue-fluorescent protein, BFP, genetically fused to the C-terminus of H2A. This fusion was unable to rescue drug resistance or restore RAD51 foci in BARD1 depleted cells (Fig. 6D, Supplemental Fig 6G & I) indicating that not all C-terminal protein fusions can complement. We addressed whether the location of the Ub might be critical and compared H2A (again bearing K to R mutations in 13, 15, 118, 119, 125, 127 & 129) in which Ub had been fused to the N-terminus, the C-terminus or both the C and N-termini. The N-terminal fusion of Ub to H2A slightly improved the numbers of RAD51 foci in BARD1 deleted cells whereas RAD51 foci in cells expressing H2A with Ub fusion to the C-terminus or to both ends were fully restored (Fig. 6D). These data suggest a C-terminal Ub fusion is most able to promote RAD51 foci formation and that Ub fused to the N-terminus is not inhibitory to the restoration of HR promoted by the C-terminal fusion. Taken together these data indicate that incorporation of H2A-Ub into chromatin either supports a function similar to that of the BRCA1-BARD1 ligase or contributes an indirect role able to overcome the need for the heterodimer activity.

We next addressed how BRCA1-BARD1 ligase activity or Ub-modified nucleosomes might

impact 53BP1 and resection. We assessed whether H2A-Ub fusions inhibit 53BP1 accumulation to IRIF, whether BRCA1-BARD1 depletion results in expression of epigenetically silenced genes or whether depletion of a repressive chromatin factor, Chromodomain Helicase DNA Binding Protein 3(CHD3), part of the repressive Nucleosome Remodeling Deacetylase complex, might relieve the requirement for BRCA1:BARD1 (Supplemental Fig 7A-F). These potential mechanisms were unsupported by evidence from these investigations.

SMARCAD1 is part of the BRCA1-BARD1 ligase pathway.

We then focused on the proteins involved in the later-stages of DNA resection and noted reduced BLM recruitment to IRIF in BARD1 depleted cells (Supplemental Figure 7G). Unlike the requirement for BRCA1-BARD1 ligase activity, the requirement for late-stage resection enzymes in HR cannot be overcome by loss of 53BP1[29,30], leading us to consider the phenomenon of poor BLM recruitment as an indication of a defect earlier in the process. In yeast the ATP-dependent chromatin remodeler Function Unknown Now 30, Fun30, acts to promote Exo1 and Sgs1/BLM in resection[31-33]. The mammalian homologue, SMARCAD1 also promotes resection [32] and the protein has two Ubiquitin-binding CUE domains (similar to a domain in the yeast Cue1 protein)[34] (Fig 7A). To test whether this protein might link BRCA1-BARD1 dependent chromatin modification to 53BP1 repositioning and DNA resection, we examined interaction of the SMARCAD1 CUE domains with H2A-Ub bearing nucleosomes. Nickel beads bound to 6xHis-tagged SMARCAD1 CUE domains were able to purify H2A-Ub, but not H2A, whereas SMARCAD1-CUE-domain mutants (with Ub-contacting F, A & L residues previously described [35] changed to E, termed CUEm) purified neither histone (Fig 7B).

We next addressed SMARCAD1 recruitment and introduced siRNA resistant plasmids encoding full-length SMARCAD1 or CUEm-SMARCAD1 into SMARCAD1 depleted cells (Fig. 7C). WT-SMARCAD1 localized to laser-induced sites of DNA damage decorated with γH2AX (Fig. 7D). Its accumulation was reduced, but not lost, when BARD1 was depleted. Similarly the CUE- mutant showed reduced intensity at laser induced sites of damage compared to the WT protein (Fig. 7D). The recruitment of CUEm-SMARCAD1 was not reduced further by depletion of BARD1 suggesting BARD1 and the CUE domains affect SMARCAD1 accumulation through the same pathway (Fig. 7D). Pre-treatment of cells with KU55933, a specific inhibitor ATM inhibitor[36], substantially diminished the formation of phosphorylated H2AX (γH2AX) from the path of the laser-line, and it also sustainably diminished SMARCAD1 accumulation (Fig. 7D). Thus although BRCA1-BARD1 and SMARCAD1 CUE domains support SMARCAD1 recruitment, other ATM-dependent events are also required.

We further tested the relationship between BRCA1-BARD1 and SMARCAD1. We found that although SMARCAD1 depletion alone reduced drug resistance and HR, this was not worsened in cells also without BRCA1-BARD1 activity (Supplemental Fig 8A &B), suggesting SMARCAD1 and BRCA1-BARD1 ligase activity influence drug resistance through the same pathway. Moreover H2A-Ub expression was unable to restore RAD51 foci levels in BARD1 depleted cells that were also depleted of SMARCAD1 (Supplemental Fig 8C). This evidence points to a requirement for SMARCAD1 down-stream of BRCA1-BARD1 ligase activity and C-terminal H2A-ubiquitination. Based on these data we predicted a similar function for SMARCAD1 in resection and HR as BRCA1-BARD1 and therefore examined the relationship with 53BP1 in resection and in IRIF. Loss of 53BP1 restored full BrdU resection lengths to SMARCAD1 depleted cells (Fig 7E)

suggesting an antagonistic relationship between SMARCAD1 and 53BP1 regulates resection. Further in S-phase or G2 cells depleted for SMARCAD1 we observed that 53BP1 was not evicted to the periphery of BRCA1-associated foci, indicating SMARCAD1 is also required for 53BP1 repositioning (Fig. 7F). Expression of an siRNA resistant WT-SMARCAD1 protein restored normal distribution of 53BP1 but expression of the CUEm-SMARCAD1 or an ATPase-dead form (K528R) did not (Fig 7F and Supplemental Fig 8D), indicating both the CUE domains and enzymatic activity are required for repositioning 53BP1. Since the impact is not partial, these data also suggest that the CUE domains have a role in promoting 53BP1 repositioning beyond supporting accumulation of SMARCAD1 to sites of damage.

In complementation of cells depleted for endogenous SMARCAD1 we found that CUEm-SMARCAD1 was unable to restore RAD51 foci in IR-treated cells and neither CUEm-SMARCAD1 nor the ATPase-dead mutant form could restore Olaparib or Camptothecin resistance of SMARCAD1 depleted cells (Fig 7G, Supplemental Fig 8E). Thus the SMARCAD1 CUE domains are vital to promote HR, correlating with their role in 53BP1 repositioning and drug resistance. As anticipated the need for the SMARCAD1 CUE-domains in promoting HR, measured by RAD51 IRIF formation, was by-passed by treatment with siRNA to 53BP1 (Fig 7G). Similarly the repression of 53BP1 restored cellular Olaparib and Camptothecin resistance in cells depleted for SMARCAD1 (Fig 7H) confirming that SMARCAD1 is less important to cell survival when 53BP1 is absent. Together these data confirm a link between BRCA1-BARD1 and SMARCAD1 in the promotion of resection in the presence of 53BP1.

Discussion.

Our data now provide some insight into how BRCA1 acts to inhibit the 53BP1-complex mediated block on resection. The BRCA1-BARD1 Ub ligase promotes a subset of DNA repair functions attributed to BRCA1 and participates in promoting resection steps after CtIP and MRE11-mediated commitment to HR. Consistent with the restoration of HR in BRCA1-BARD1 deficient cells, we find that H2A-Ub complementation functions at the level of resection restoration. Initially we were surprised that our data indicates that C-terminal Ub modification of H2A is unlikely to directly inhibit the 53BP1 interactions. Instead we show that promotion of HR requires the Ub-binding CUE domains of the chromatin remodeler SMARCAD1. Critically both BRCA1 ligase activity and SMARCAD1 act to reposition 53BP1 within IRIF, correlating with the promotion of resection.

Our data suggest to us a model in which the BRCA1-BARD1 ligase modifies chromatin which in turn promotes the accumulation and activity of the chromatin remodeler SMARCAD1 which then acts to mobilize 53BP1, allowing the completion of resection (Fig 8). By this means we suggest that BRCA1 activity promotes HR and inhibits toxic end-joining. Our model does not exclude an additional role for the 53BP1 ubiquitination that we observe but we note that H2A-Ub is sufficient to restore HR to near normal levels in BRCA1-BARD1 deficient cells.

Yeast Fun30 can both slide nucleosomes and evict histone H2A and H2B dimers[37,38] so that whether SMARCAD1 shunts or removes DNA-damage proximal histones is not yet known. Conceptually, nucleosome sliding may be inhibited by upstream nucleosomes and eviction is a simpler model. In yeast histones remain bound to DSB ends longer in *fun30*Δ cells[31]. In either case, remodeled nucleosomes may be those loaded with 53BP1, or become refractory to 53BP1 interaction. SMARCAD1 is also required in the re-establishment of silent

heterochromatin after DNA replication[39]. It will be intriguing to discover whether reduced SMARCAD1 activity at chromatin contributes to the reduced heterochromatin observed in Brca1 deficient murine cells[9].

We have shown that cell survival in response to some DNA damaging agents requires BRCA1 ligase function to counter 53BP1, whereas the responses to other agents, which induce replicative stress or intra-strand cross-links, are independent of this pathway. This information may provide a rationale for tailored anticancer treatment for some *BRCA1* mutation carriers since targeting ligase-dependent and independent aspects of the BRCA1 defect would be expected to slow the development of tumor resistance through 53BP1- complex down-regulation or mutation.

Several *BRCA1* patient missense variants occur in the N-terminus with the potential to disrupt E3 Ub ligase function[16]. The role we have identified for the ligase activity in promoting HR is suggestive of a role in cancer protection. In defining the Ub-priming face of this and other Type-1 E3 Ub ligases our data provide a robust and novel means by which the ligase function can be assessed in cells and organisms.

Acknowledgements

Grant funding for this project was as follows. CRUK: C8820/A19062 (RMD, AG, HS, JB), C302/A14532 and C1206/A11978 (FZW, LHP), Breast cancer Campaign: 2010MayPR01 (JS), 2013NovPR132 (S B-R). Engineering and Physical Sciences Research Council EP/L016346/1 (RN), University of Birmingham (AF, BJ and RMD). University of Sussex (RB): JRM, RN and NHK are HEFCE funded.

We thank J. Stark (City of Hope) for U20S-DR3 and U20S-EJ5 cells and *I-SCE1* plasmid, R. Everett, MRC Virology Unit, Glasgow for UBE2D1 cDNA, and Myc-His-Ubiquitin construct. T.Sixma and M. van Lohuizen, (both NKI Netherlands) for Ring1b$_{159}$/Bmi1$_{109}$ co-expression construct and BMI1-GFP. R. Goodman, Vollum Institute, Portland, OR. HA-Rad18 was a kind gift from A. Zlatanou and the Flp-In^{TM} Hela cells and MDC1 antibody were a generous gift from G. Stewart, both University of Birmingham, UK. R. Katz (Fox Chase Cancer Centre, Philadelphia, PA, USA) for cryptic EGFP Hela cells and J. Tainer (The Scripps Research Institute, CA, USA) for PFM01 inhibitor. Determination of the structure of the TRIM37 domain was supported by an NIH Protein Structure Initiative grant to G.T. Montelione, J.F. Hunt, and the Northeast Structural Genomics Consortium. We thank R. Hay for useful discussions and T. Sixma and M. Uckelmann for insights into the contribution of H2A-Ub interactions in purified nucleosomes.

Author Contributions

RMD performed structural analysis, generated proteins, performed cell and biochemical experiments, designed experiments and interpreted data. AG generated constructs and cell lines, and performed colony survival experiments. HS performed resection experiments and fluorescence microscopy. JS generated BARD1 cell lines and undertook immunoprecipitation experiments, RB performed high resolution BRCA1 and 53BP1 microscopy and analysis. AF generated RING1B-BMI1 proteins and performed biochemistry, BJ undertook foci quantitation. M D-M generated BRCA1 cell lines. S B-R and JB provided technical support and yeast experiments. LHP, RN, NHK and FW provided supervisory help and data interpretation. JRM and RMD wrote the paper. AG, HS and M D-M commented on the paper and on-going research. JRM contributed to data interpretation and directed the project.

References.

1. Long, D.T. & Walter, J.C. A novel function for BRCA1 in crosslink repair. *Molecular cell* **46**, 111-2 (2012).
2. Schlacher, K., Wu, H. & Jasin, M. A distinct replication fork protection pathway connects Fanconi anemia tumor suppressors to RAD51-BRCA1/2. *Cancer Cell* **22**, 106-16 (2012).
3. Jiang, Q. & Greenberg, R.A. Deciphering the BRCA1 Tumor Suppressor Network. *J Biol Chem* **290**, 17724-32 (2015).
4. Panier, S. & Boulton, S.J. Double-strand break repair: 53BP1 comes into focus. *Nat Rev Mol Cell Biol* **15**, 7-18 (2014).
5. Bunting, S.F. et al. 53BP1 inhibits homologous recombination in Brca1-deficient cells by blocking resection of DNA breaks. *Cell* **141**, 243-54 (2010).
6. Escribano-Diaz, C. et al. A cell cycle-dependent regulatory circuit composed of 53BP1-RIF1 and BRCA1-CtIP controls DNA repair pathway choice. *Mol Cell* **49**, 872-83 (2013).
7. Brzovic, P.S. et al. Binding and recognition in the assembly of an active BRCA1/BARD1 ubiquitin-ligase complex. *Proc Natl Acad Sci U S A* **100**, 5646-51 (2003).
8. Kalb, R., Mallery, D.L., Larkin, C., Huang, J.T. & Hiom, K. BRCA1 is a histone-H2A-specific ubiquitin ligase. *Cell reports* **8**, 999-1005 (2014).
9. Zhu, Q. et al. BRCA1 tumour suppression occurs via heterochromatin-mediated silencing. *Nature* **477**, 179-84 (2011).
10. Sato, K. et al. A DNA-damage selective role for BRCA1 E3 ligase in claspin ubiquitylation, CHK1 activation, and DNA repair. *Current biology : CB* **22**, 1659-66 (2012).
11. Reid, L.J. et al. E3 ligase activity of BRCA1 is not essential for mammalian cell viability or homology-directed repair of double-strand DNA breaks. *Proc Natl Acad Sci U S A* **105**, 20876-81 (2008).
12. Drost, R. et al. BRCA1 RING Function Is Essential for Tumor Suppression but Dispensable for Therapy Resistance. *Cancer Cell* **20**, 797-809 (2011).
13. Plechanovova, A. et al. Mechanism of ubiquitylation by dimeric RING ligase RNF4. *Nature structural & molecular biology* **18**, 1052-9 (2011).
14. Dou, H., Buetow, L., Sibbet, G.J., Cameron, K. & Huang, D.T. Essentiality of a non-RING element in priming donor ubiquitin for catalysis by a monomeric E3. *Nature structural & molecular biology* (2013).
15. Metzger, M.B., Pruneda, J.N., Klevit, R.E. & Weissman, A.M. RING-type E3 ligases: Master manipulators of E2 ubiquitin-conjugating enzymes and ubiquitination. *Biochimica et biophysica acta* (2013).
16. Morris, J.R. et al. Genetic analysis of BRCA1 ubiquitin ligase activity and its relationship to breast cancer susceptibility. *Hum Mol Genet* **15**, 599-606 (2006).
17. Mallery, D.L., Vandenberg, C.J. & Hiom, K. Activation of the E3 ligase function of the BRCA1/BARD1 complex by polyubiquitin chains. *Embo J* **21**, 6755-62 (2002).
18. Brzovic, P.S., Rajagopal, P., Hoyt, D.W., King, M.C. & Klevit, R.E. Structure of a BRCA1-BARD1 heterodimeric RING-RING complex. *Nature structural biology* **8**, 833-7 (2001).
19. Ismail, I.H., McDonald, D., Strickfaden, H., Xu, Z. & Hendzel, M.J. A small molecule inhibitor of polycomb repressive complex 1 inhibits ubiquitin signaling at DNA double-strand breaks. *The Journal of Biological Chemistry* **288**, 26944-54 (2013).
20. Morris, J.R., Keep, N.H. & Solomon, E. Identification of residues required for the interaction of BARD1 with BRCA1. *J Biol Chem* **277**, 9382-6 (2002).
21. Boersma, V. et al. MAD2L2 controls DNA repair at telomeres and DNA breaks by inhibiting 5' end resection. *Nature* (2015).
22. Xu, G. et al. REV7 counteracts DNA double-strand break resection and affects PARP inhibition. *Nature* (2015).
23. Wang, J. et al. PTIP associates with Artemis to dictate DNA repair pathway choice. *Genes Dev* **28**, 2693-8 (2014).
24. Chapman, J.R., Sossick, A.J., Boulton, S.J. & Jackson, S.P. BRCA1-associated exclusion of 53BP1 from DNA damage sites underlies temporal control of DNA repair. *Journal of cell science* (2012).
25. Kakarougkas, A. et al. Co-operation of BRCA1 and POH1 relieves the barriers posed by 53BP1 and RAP80 to resection. *Nucleic acids research* **41**, 10298-311 (2013).
26. Cejka, P. DNA End Resection: Nucleases Team Up with the Right Partners to Initiate

Homologous Recombination. *J Biol Chem* **290**, 22931-8 (2015).
27. Cruz-García, A., López-Saavedra, A. & Huertas, P. BRCA1 Accelerates CtIP-Mediated DNA-End Resection. *Cell Reports* **9**, 451-459 (2014).
28. Shibata, A. et al. Role of ATM and the damage response mediator proteins 53BP1 and MDC1 in the maintenance of G(2)/M checkpoint arrest. *Mol Cell Biol* **30**, 3371-83 (2010).
29. Tomimatsu, N. et al. Exo1 plays a major role in DNA end resection in humans and influences double-strand break repair and damage signaling decisions. *DNA Repair (Amst)* **11**, 441-8 (2012).
30. Grabarz, A. et al. A role for BLM in double-strand break repair pathway choice: prevention of CtIP/Mre11-mediated alternative nonhomologous end-joining. *Cell reports* **5**, 21-8 (2013).
31. Chen, X. et al. The Fun30 nucleosome remodeller promotes resection of DNA double-strand break ends. *Nature* **489**, 576-80 (2012).
32. Costelloe, T. et al. The yeast Fun30 and human SMARCAD1 chromatin remodellers promote DNA end resection. *Nature* **489**, 581-4 (2012).
33. Eapen, V.V., Sugawara, N., Tsabar, M., Wu, W.H. & Haber, J.E. The Saccharomyces cerevisiae chromatin remodeler Fun30 regulates DNA end resection and checkpoint deactivation. *Mol Cell Biol* **32**, 4727-40 (2012).
34. Neves-Costa, A., Will, W.R., Vetter, A.T., Miller, J.R. & Varga-Weisz, P. The SNF2-family member Fun30 promotes gene silencing in heterochromatic loci. *PLoS ONE* **4**, e8111 (2009).
35. Shih, S.C. et al. A ubiquitin-binding motif required for intramolecular monoubiquitylation, the CUE domain. *Embo J* **22**, 1273-81 (2003).
36. Hickson, I. et al. Identification and characterization of a novel and specific inhibitor of the ataxia-telangiectasia mutated kinase ATM. *Cancer Res* **64**, 9152-9 (2004).
37. Byeon, B. et al. The ATP-dependent chromatin remodeling enzyme Fun30 represses transcription by sliding promoter-proximal nucleosomes. *J Biol Chem* **288**, 23182-93 (2013).
38. Awad, S., Ryan, D., Prochasson, P., Owen-Hughes, T. & Hassan, A.H. The Snf2 homolog Fun30 acts as a homodimeric ATP-dependent chromatin-remodeling enzyme. *J Biol Chem* **285**, 9477-84 (2010).
39. Rowbotham, S.P. et al. Maintenance of silent chromatin through replication requires SWI/SNF-like chromatin remodeler SMARCAD1. *Mol Cell* **42**, 285-96 (2011).
40. Buchwald, G. et al. Structure and E3-ligase activity of the Ring-Ring complex of polycomb proteins Bmi1 and Ring1b. *The EMBO journal* **25**, 2465-74 (2006).
41. Huang, A. et al. Symmetry and asymmetry of the RING-RING dimer of Rad18. *J Mol Biol* **410**, 424-35 (2011).
42. Kuzin, A., Chen, Y., Seetharaman, J., Mao, M., Xiao, R., Ciccosanti, C., Shastry, R., Everett, J.K., Nair, R., Acton, T.B., Rost, B., Montelione, G.T., Tong, L., Hunt, J.F.
43. Kappo, M.A. et al. Solution structure of RING finger-like domain of retinoblastoma-binding protein-6 (RBBP6) suggests it functions as a U-box. *J Biol Chem* **287**, 7146-58 (2012).

Figure Legends.

Uncropped blot images can be found in Supplementary Data Set 1 and source data for the graphs can be found in Supplementary Source Files Figs 1-7.

Figure 1. A basic residue of BARD1 promotes Ub-transfer from BRCA1-E2~Ub

A. Western blots comparing the ability of BRCA1-BARD1 heterodimer containing Wild type (WT) WT-BARD1 or R99E-BARD1 to catalyse the formation of Ub chains. Ub mix refers to E1, E2, Ub, ATP and ligase reaction buffer. Probed for BRCA1, 6xHis (BARD1) and Ub.
B. Yeast two hybrid assays showing the BRCA1-BARD1 heterodimer is not disrupted by BARD1-R99 variants. Yeast strains expressed VP16-BRCA1 1-300 with WT and substituted LexA-BARD1 27-146 (100 mM 3AT). L44R is included as a heterodimer-disruptive control [19].

C. Top, western blots showing improved activity of R99E-BARD1 heterodimer with D32R mutant Ub. Graph below shows quantification of high molecular weight Ub from 4 independent experiments, bars are s.e.m (Note R99E-heterodimer reaction exposed longer than control). * indicates $p<0.05$, Student's t-test throughout.

D. *In vitro* assays showing ability of WT and R99E-BARD1 heterodimers to discharge Ub from a loaded E2~Ub dimer. Results show mean and s.e.m from 4 independent experiments.

Figure 2. Other Type-I RING E3 ligases require R or K residues on the partner protomer.

A. Structural models showing views in the same orientation of Type 1 RING:RING structures: BRCA1-BARD1 (PDB: 1JM7 ref 18) with BMI1-RING1B (PDB: 2CKL ref 40), RAD18 (PDB:2Y43 ref 41), TRIM37 (PDB:3LRQ[42]), and RBBP6 (PDB:3ZTG ref [43]), residues equivalent to R99-BARD1 are shown in pink.

B. Western blot indicating the ability to induce mono-ubiquitination of PCNA is lost by R76A-RAD18. Cells transfected with either WT-RAD18 or R76A-RAD18 mutant in otherwise untreated 293 cells or those treated with 40 J UV. Lysates were probed for PCNA and controls as shown.

C. Western blots indicating mono-ubiquitination of H2A in nucleosomes by incubation with WT BMI1-RING1B and K73E-BMI1 bearing RING1B heterodimer.

Figure 3. BRCA1-BARD1 ligase activity promotes survival to a subset of DNA damaging agents.

A. Structural model BARD1 (orange) and BRCA1 (green) (PDB: 1JM7) illustrating the location of L44 (blue) and R99 (pink) residues. Zinc ions are filled spheres (black). Lower image is 90^{o} rotation about the horizontal.

B. Immunoblot of cells treated with Non-targeting control siRNA (NTC) or BARD1 siRNA and complemented with siRNA-resistant BARD1 variants shown. The graphs show cell survival relative to NTC control of cells depleted and complemented in this way were exposed to the agents shown, plated and clones counted 10-14 days later. Colony numbers are expressed as % of untreated cells. 4 replicates per experiment and means from minimum of 3 experiments shown, bars are s.e.m.

C. As in B, depleted with siRNA to BRCA1 and complemented with siRNA resistant WT-BRCA1 and I26A-BRCA1. 4 replicates per experiment, 4 experiments, bars are s.e.m.

Figure 4. BRCA1-BARD1 ligase activity promotes DNA resection in the presence of 53BP1.

A. RPA and RAD51 foci in EdU positive cells treated with BARD1 siRNA and complemented with siRNA resistant WT, R99E- or L44R-BARD1 variants. Images show representative cells. Scale bars are 10 μm throughout. Graphs (right) show the mean number of foci per cell RPA = 60 cells, Rad51 = 100 cells, bars are s.e.m. ***$p<0.005$.

B. The graph shows colony cell survival in Olaparib (10 μM) relative to NTC control of cells treated with BARD1 siRNA and complemented with WT or R99E-BARD1 and treated with additional siRNAs shown. 3, replicates per experiment, 4 experiments, bars are s.e.m. *$p<0.05$. Western blots (right) show detection of BARD1, CtIP and 53BP1 in treated cells.

C. Graph shows colony survival of BRCA1 depleted cells and cells co-depleted with 53BP1 and treated with Hydroxyurea (3 mM) relative to NTC treated controls. 3 replicates per

experiment, 3 experiments, bars are s.e.m. * indicates p<0.05. Western blots (right) show detection of 53BP1, BRCA1 in treated cells.

D. High-resolution images of BRCA1 and 53BP1 in cells treated with BARD1 siRNA and complemented with WT- or R99E-BARD1, exposed to 2 Gy IR and fixed 8 hours later. An average across 30 profiles is shown, over 3 experimental repeats. Bars =1 standard deviation.

Figure 5. BRCA1-BARD1 ligase activity is required after HR-commitment.

A. BrdU track lengths in cells were treated with BrdU, and Olaparib (10 μM). 50 fibres, horizontal line represents mean, bars= s.e.m. ***p<0.005.

B. Graph shows quantification of GFP recovery in NHEJ-substrate cells depleted for BARD1 and transfected with siRNA resistant variants, 3 replicates per experiment, 4 experiments, bars are s.e.m ***= p<0.005.

C. Graph shows quantification of GFP recovery in NHEJ-substrate cells depleted for BARD1, CtIP or both 3 replicates per experiment, 6 experiments, bars are s.e.m ***= p<0.005.

D. Graph shows quantification of GFP recovery in HR-substrate cells depleted for BARD1, CtIP or both. 3 replicates per experiment, 6 experiments, bars are s.e.m ***= p<0.005.

E. Graph shows colony survival of cells treated with IR (0.5 Gy) and depleted for BARD1 and complemented with WT or R99E-BARD1 or co-depleted for BARD1 and CtIP relative to control treated cells. 3 replicates per experiment, 3 experiments, bars are s.e.m ***= p<0.005.

Figure 6. BRCA1-BARD1 dependent modification of nucleosomes.

A. Western blot of selected proteins in whole cell extracts (WCE) and Nickel-column precipitations (Ni^{2+} IP) of lysates from cells transfected with His-Myc-Ub and BARD1 constructs and irradiated (30 Gy).

B. Western blot of HA-H2A of cells transfected with HA-H2A or HA-H2A-Ub fusion. In the fusion Histone 2A carried lysine to arginine mutations at lysines K13 15 118 119 125 127 and 129 and in the Ub the seven lysines of Ub were mutated to R (illustrated top). Cells were lysed sequentially in buffer containing increasing amounts of salt. Sol = soluble fraction Nuc= nuclear fraction and Pel= Pellet.

C. Quantification of HA-H2A-Ub intensity (expression) and number of RAD51 foci in BARD1 depleted S-phase cells after exposure to IR (5 Gy) and 2 hours recovery (for representative immunofluorescence images see Supplemental Fig 6E) n=30 cells. Western blots (right) shows BARD1 and HA-H2A-Ub expression in treated cells.

D. Graph below shows quantification of RAD51 foci in BARD1 depleted cells expressing HA-H2A or various fusions of H2A and pulsed with EdU fixed 2 hours after 5 Gy IR. n=75 cells per condition from 3 experiments, bars= s.e.m. Images top show cells stained with RAD51, HA and incubated with click-it detection reagents to detect EdU labelled S-phase cells.

Figure 7. The nucleosome remodeler SMARCAD1 is in the same pathway as BRCA1-BARD1 ligase activity.

A. Illustration of SMARCAD1 protein.
B. Western blot showing the detection of HA-H2A (WT) or H2A-Ub expressed in cells and bound, or not bound, to *in vitro* purified WT or mutant SMARCAD1 CUE domains (amino acids 98-318).
C. Western blot showing expression of full length WT and CUE-domain mutant SMARCAD1 in SMARCAD1 depleted cells.
D. Representative images (left) of cells expressing siRNA resistant SMARCAD1 variants treated with SMARCAD1 siRNA or co-depleted with siRNA to BARD1 and bearing laser-line induced DNA damage. Cells labelled ATMi = 10 μM KU55933 ATM inhibitor 4 hours prior to damage. White 'X' marks the laser-line path. The graph shows intensity of myc-SMARCAD1 measured in the region of the γH2AX laser line compared to nucleoplasm intensity. 25 lines per experiment, 2 experiments, bars S.E. **= $p<0.05$, ***= $p<0.005$ Student t-test. Scale bars 10 μm
E. Length of BrdU DNA fibres after treatment with Olaparib (10 μM) in cells treated with the siRNAs shown. Western blots (right) shows detection of BARD1 and SMARCAD1 proteins in treated cells.
F. Representative images (left) of cells transfected with siRNA targeting SMARCAD1 with siRNA resistant WT and CUEm myc-SMARCAD1 exposed to 2 Gy IR and fixed 8 hours later. Graphs (right) show averages of 30 foci profiles over 3 experimental repeats. Bars =1 standard deviation.
G. Quantification RAD51 foci in cells transfected with SMARCAD1 and 53BP1 siRNA together with siRNA resistant forms of SMARCAD1, n=70 cells, bars= s.e.m. ***$p<0.005$).
H. The graph shows colony cell survival in Olaparib (10 μM) and Camptothecin (2.5 μM) relative to NTC control of SMARCAD1 complemented cells, 3 replicates per experiment, 6 experiments, bars are s.e.m. $p<0.005$. Western blots (right) show detection of SMARCAD1 and 53BP1 in treated cells.

Figure 8. Proposed model for the BRCA1-BARD1 Ub ligase in promoting resection at DSB-damaged chromatin.

1. Limited resection occurs in the absence of BRCA1-BARD1 activity dependent on CtIP-Mre11.
2. BRCA1-BARD1 dependent Ub modification of H2A promotes SMARCAD1 interaction with damage-proximal nucleosomes.
3. SMARCAD1 activity to reposition or evicts nucleosome, and move 53BP1 and its effector proteins to release 53BP1-mediated inhibition of DNA resection.
4. Long range resection can proceed.

Online Methods

Western blots show a representative image taken from >3 independent experiments unless otherwise specified. A full list of primers, siRNA sequences and antibodies used can be found in Suppl. Tables 1-3. All constructs and mutations generated in-house by site-directed mutagenesis were confirmed by sequencing (Source Biosciences). All chemicals, unless otherwise stated are from Sigma or Fisher.

Yeast Two and Three hybrid Assays. The yeast expression vectors used contained human BRCA1-N-terminal amino acids 2–300 expressed as a fusion with the transactivation domain VP16 (pVP16-BRCA1), and full length E2 ubiquitin conjugating enzyme, human UBE2D1, or BARD1 amino acids 27-146, expressed as fusions with the DNA-binding protein LexA (pLexA). For three-hybrid studies pY3H-Ade2 was generated from pY3H (Dualsystems Biotech) by cloning the Ade2 gene into Sbf1 and Stu1 sites which resulted in destruction of the original Ura2 selection gene. Full length BARD1 was cloned into pY3H-Ade2 vector by Genscript. Growth on increasing concentrations of 3-Amino-1,2,4-triazole (3-AT) a competitive inhibitor of the product of the HIS3 gene, indicate greater transcriptional production of HIS3.

BRCA1-BARD1 protein production. For bacterial expression of human BRCA1:BARD1 heterodimer a bi-cistronic expression vector encoding six histidine-tagged BRCA1 amino acids 1–300 and six histidine-tagged BARD1 amino acids 26–142 was generated by amplification of human BRCA1 and BARD1 cDNA templates and cloned into pET15b. Mutations were made by site-directed mutagenesis in BRCA1 or BARD1. Proteins were purified as described previously [16]. In brief, BRCA1 and BARD1 proteins were expressed in BL21-DE3 bacteria (Bioline). Bacteria were grown at 37 ^{o}C until optical density 0.6 was reached. Protein expression was induced by addition of 0.5 mM Isopropyl β-D-1-thiogalactopyranoside (IPTG)(Bioline) and the temperature immediately reduced to 25 ^{o}C. Bacteria were grown for a further 24 hours. A bacterial pellet was collected following centrifugation at 3000g for 10 min, 4 ^{o}C and then lysed in ice cold lysis buffer (50 mM sodium phosphate, pH7, 300 mM sodium chloride, 5 % glycerol, 10 mM beta-mercaptoethanol). The lysate was sonicated for 1 min at 30 % intensity and then clarified by centrifugation at 14,000 g, 10 min, 4 ^{o}C. The supernatant was incubated with 0.25 ml His-select beads (Sigma) overnight at 4 ^{o}C with rotation. The following day the beads were washed with three ten minute washes in ice cold wash buffer (50 mM sodium phosphate, pH7, 300 mM sodium chloride, 5 % glycerol, 10 mM beta-mercaptoethanol, 50 mM imidazole) before eluting on ice in elution buffer (50 mM sodium phosphate, pH7, 300 mM sodium chloride, 5 % glycerol, 10 mM beta-mercaptoethanol, 300 mM imidazole) . Purified proteins were dialyzed against (25 mM TRIS-HCl, pH7.5, 10 % glycerol, 2 mM dithiothreitol (DTT), 150 mM potassium chloride) and purity checked by resolution on 15% SDS-PAGE gel.

BMI1-RING1B protein production. Ring1b$_{159}$-Bmi1$_{109}$ construct (a kind gift of Titia Sixma, NKI Netherlands) was co-expressed in *E. coli* BL21 (DE3) with both genes on a single promoter and a glutathione-*S*-transferase (GST) fusion tag on the RING1B fragment only. After co-purification on Glutathione Sepharose columns and washing, the dimer was eluted by cleaving with PreScission protease (after Buchwald *et al* 2006 [40]). Protein purity was checked by resolution on 15% SDS-PAGE gel.

Wild-type and D32R-Ub protein production. Synthetic yeast ubiquitin was cloned into pGEX2TK, before site directed mutagenesis to generate D32R. Constructs were expressed in BL21 cells (Bioline) and grown at 37 ^{o}C to an OD of 0.6 before inducing protein expression with 0.5 mM IPTG. Bacteria were grown for a further 16 hours before lysis (20 mM Tris-HCl pH 8, 130 mM sodium chloride, 1 mM EGTA, 1.5 mM magnesium chloride, 1 % Triton x100, 10% glycerol, 1 mM DTT and Protease Inhibitors (Complete Protease Inhibitor tablets – Roche). The lysate was sonicated for 1 min at 30 % intensity and then clarified by centrifugation at 14,000 g, 10 min, 4 ^{o}C. The supernatant was incubated with 0.25 ml glutathione sepharose-4B beads

(GE Healthcare) overnight at 4 ^{o}C with rotation. The following day the beads were washed with three ten minute washes in ice cold lysis buffer before a final wash in thrombin cleavage buffer (20 mM TRIS pH 8.4, 150 mM sodium chloride, 2.5 mM calcium chloride). Ubiquitin was eluted from the beads by cleaving the GST-tag with 2 Units of thrombin (Promega) overnight at 4 ^{o}C. The following day the supernatant was incubated with 50 ul p-aminobenzamidine-agarose (Sigma) for 2 hours to remove Thrombin before dialysis against (25 mM TRIS-HCl, pH7.5, 10 % glycerol, 2 mM dithiothreitol (DTT), 150 mM potassium chloride).

SMARCAD1-CUE domain protein production and pull downs. Codon optimized SMARCAD1-CUE domains (amino acids 98-318) WT and CUEm (L168E F169E L195E L196E F263E A285E L286E) were custom synthesized by Genscript and sub-cloned into pET15b. The CUE domains were expressed in BL21-DE3 bacteria and purified onto Nickel beads as described for BRCA1-BARD1 protein production. Nickel beads bound by CUE domains were stored in PBS for short term pull down experiments.
Lysates were prepared from HeLa Flp In stable cell lines (Empty, HA-H2A or HA-H2A-Ub cell lines) which had been induced with Doxycycline (1 μg/ml) for 72 hours to allow protein expression and chromatin incorporation of the HA-H2A constructs. Cells were lysed in 20 mM Tris pH8, 137 mM NaCl, 1 mM EGTA, 1.5 mM $MgCl_2$, 1 % TritonX100, 10 % Glycerol with the addition of Protease Inhibitors (Complete Tablets – Roche), Phosphatase Inhibitors (PhosSTOP – Roche), 10 mM Iodoacetimide and 4 mM N-Ethylmaleimide. DNAse1 (0.1 mg/ml) was added for 30 mins on ice before centrifugation and incubation with His-beads or His-CUE domain beads overnight at 4 ^{o}C. Samples were washed 4x with ice-cold PBS, resuspended in SDS-PAGE loading buffer and resolved by western blotting.

Ubiquitin ligase assays. Ubiquitin conjugation assays were performed as described [44]. Ligase assays were carried out in 50 mM Tris-HCl (pH 7.5), 50 mM sodium chloride, 5 mM ATP. The precise concentrations of the proteins and the reaction conditions used varied over the following ranges: 100 ng E1, 25 ng UBE2D1-3 enzymes (Viva Biosciences, Exeter UK) and 2.5 μg ubiquitin (Sigma), and ~ 30 ng of ligase proteins. The mixtures were incubated at 37°C (BRCA1-BARD1) or 30°C (BMI1-RING1B) for 30 to 60 min and then stopped with 3x gel-loading buffer, subjected to electrophoresis and western blotting for Ubiquitin (P4D1) and BRCA1 (MS110). Note for comparison of WT and R99E-BARD1 containing heterodimers, with mutant D33R Ub the WT complexes were incubated for 15 minutes, the mutant reactions for 1 hour. In reactions examining nucleosome modification 0.05 μg nucleosomes (Cambridge Bioscience) was added per reaction as described above.

Ub-Transfer Reactions. E2 (UBE2D1, 3) was first charged with ubiquitin in the absence of an E3 and a substrate. To prepare the UBE2D1~Ub thioester, we incubated UBE2D1 and ubiquitin (both 100 μM) with 0.2 μM Ube1 in 50 mM Tris, 150 mM NaCl, 3 mM ATP, 5 mM $MgCl_2$, 0.5 mM TCEP and 0.1% (v/v) NP40 (pH 7.5) at 37 °C for 12 min. To stop E1-mediated loading of E2 with ubiquitin, we depleted ATP by adding apyrase (4.5 U ml−1; New England BioLabs). The E2~Ub thioester (~20 μM) was incubated with BRCA1-BARD1, ~ 30 ng, and 500 mM lysine at room temperature. Reactions were stopped by addition of non-reducing SDS-PAGE loading buffer. The percentage of E2 modified with ubiquitin was determined by quantification of scans using ImageJ software. Reaction time points were taken from 30 s to up to 20 min, and reaction rates were determined using at least three time points within the linear range of the

reaction.

Interrogation of protein structures. The RING domain of BRCA1 (PDB 1JM7 chain A)[18] was superimposed on the RING domain of RNF4 RING–UBE2D1(S22R/C85K)–Ub complex (PDB 4AP4)[13] using Swiss PDB-viewer. Structural representations and models were generated using PyMol (Schrödinger). Similarly the RING domain of BARD1 (PDB 1JM7 chain B) was superimposed on the RING domains of BMI1-RING1B (PDB: 2CKL)[40], RAD18 (PDB: 2Y43)[41], TRIM37 (PDB:3LRQ)[42] and RBBP6 (PDB:3ZTG)[43] to identify residues similarly located to BARD1-R99.

Cell lines. Flp-In™ Doxycyclin inducible Hela parent cell line was a kind gift of G. Stewart, University of Birmingham UK and Flp-In™ T-Rex Doxycyclin inducible 293 cell lines (Life Technologies) were grown in DMEM (Sigma), 10 % Tetracycline-Free Fetal Calf serum (Clontech) supplemented with 1 % penicillin/streptomycin. All other cell lines were grown in DMEM supplemented with 10% fetal calf serum (Sigma) and 1 % pen/strep. The pCMV-EGFP and pEF-GFP HeLa cell lines were a kind gift of R. Katz (Fox Chase Cancer Centre, Philadelphia, PA, USA). The 293T cells have been authenticated at source, the HeLa lines have not. Mycoplasma testing by Hoechst DNA staining.

BARD1 expressing lines: pcDNA5/FRT/TO-RFP-Flag-BARD1 (human) was engineered to carry silent mutations to confer siRNA resistance (WT seq: TGGTTTAGCCCTCGAAGTAAG; siRNA resistant sequence: TGGTTTtcgCCaCGtAGTAAG) and was synthesized by Genscript for WT and L44R variants. The R99E mutation was later introduced by site-directed mutagenesis and confirmed by sequencing. Stable cell lines containing Tet-inducible RFP-Flag-BARD1 were generated in Flp-In™ Hela and 293 cells by co-transfection of the pcDNA5/FRT/TO-RFP-Flag-BARD1 constructs with the recombinase pOG44 (Invitrogen) using FuGene6 (Promega). After 48 hours, cells were placed into Hygromycin selection media (400 μg/ml) and grown until colonies formed on plasmid-transfected plates but not controls. For protein expression cells were incubated +/- Doxycyclin (1 μg/ml) for 48 hours and positive clones were selected by screening for Flag expression by western blot. Expression level in the clonal cell population was confirmed by immunofluorescence for RFP. Flp-In™ 293 T-REx inducible cells expressing BARD1 derivatives were generated from pcDNA5-RFP-Flag-BARD1, recombined as described.

BRCA1 expressing lines: Flag-EGFP-BRCA1 (human) inducible Flp-In™ Hela cells expressing WT and BRCA1 mutants were generated by cloning Flag-EGFP-BRCA1 into pcDNA5/FRT/TO, before recombination and selection as described for BARD1 expressing lines.

H2A-Ub fusion expressing lines. Human HIST1H2AC was cloned in frame with an N terminal HA tag in pCDNA3.1+ by GenScript. Where indicated, individual lysines were mutated to arginine residues by gene synthesis. Human ubiquitin (UBA52) was positioned at the N terminus and/or C terminus of H2A with the addition of N terminal HA tags. cDNA for ubiquitin was mutated at each of the seven lysine residues to arginine to prevent chain formation. The sequence of all constructs was verified by GenScript. Flp-In™ Hela cells expressing H2A mutations and fusions were generated by cloning into pcDNA5/FRT/TO, (H2A-WT using HindIII:Xho1 and H2A-Ub using Hind III: BamH1), H2A-BFP was cloned directly into pcDNA5, before recombination and selection as described for BARD1 expressing lines.

Myc-SMARCAD1 expressing lines. Human SMARCAD1 cDNA was cloned in frame with a N terminal myc tag into pCDNA5/FRT/TO by gene synthesis (GenScript). The cDNA was rendered siRNA resistant to the two siRNA used in this study with the following silent mutations (indicated in red).

siRNA #1 resistance

gaa aga gat gta gtt ata agg ctt atg aac
451 E R D V V I R L M N
gaa aga gac gtc gtc att cgc ctg atg aac
451 E R D V V I R L M N

siRNA #2 resistance

agc caa ggg acg att gaa gaa tcc atg cta a
981 S Q G T I E E S M L
agc caa ggc aca atc gag gag agc atg cta a
981 S Q G T I E E S M L

The following mutations were introduced to generate the CUE 1+2 mutant; L168E, F169E, L195E, L196E (CUE1) and F263E, A285E, L286E (CUE2). The ATPase mutant (K528R) was made by site-directed mutagenesis and confirmed by sequencing.

Transfections. siRNA transfections were carried out using Dharmafect1 (Dharmacon) and DNA plasmids using FuGENE 6 (3 µl:1 µg FuGENE:DNA) (Promega) following the manufacturer's guidelines.

DNA repair reporter assays. DR3 and EJ5 U20S reporter cell lines were simultaneously co-transfected with siRNA using Dharmafect1 (Dharmacon) and DNA (RFP or RFP-BARD1 and *I-Sce1* endonuclease expression constructs) using FuGene6 (Promega) respectively. After 16 hours the media was replaced and cells were grown for a further 48 hours before fixation in 2% PFA. RFP and GFP double positive cells were scored by FACS analysis using a CyAn flow cytometer and a minimum of 10000 cells counted. Data was analyzed using Summit 4.3 software. Each individual experiment contained 3 technical repeats and normalized to siRNA controls or to WT-complemented cells. Graphs shown are combined data from a minimum of 3 independent experiments and error bars show standard error. H2A and H2A-Ub fusion constructs were co-transfected with *I-Sce1* and RFP as a surrogate marker for transfection efficiency.

Colony Assays. Cells were plated at 2 x 10^5 cells/ml in a 24 well plate and treated as required. Cells were then trypsinized transferred to a 6 well plate (volume transferred based on plating density experiments). Plates were incubated for 10-14 days. Colonies were stained using 0.5% crystal violet (BDH Chemicals) in 50% methanol and counted. Each individual experiment contained 3 technical repeats and is normalized to untreated controls. Graphs shown are combined data from a minimum of 3 independent experiments and error bars show standard error.

DNA damaging agent exposures: Cells were exposed to irradiation using a Gamma-cell 1000 Elite irradiator (caesium-137 source). Cells were exposed to Hydroxyurea overnight before

plating. For all other drugs, cells were exposed for 2 hours. Camptothecin, etoposide, 4AN, hydroxyurea, aphidicolin, and cisplatin were from Sigma. Olaparib was from Selleck chemicals.

Laser Microirradiation. Laser-microirradiation experiments were performed on BrdU-presensitized cells (10μM BrdU, 24h) as described[45] using a Zeiss PALM MicroBeam equipped with a 355 nm UV-A pulsed-laser and the 40 x objective with laser output at 40%, assisted by the PALMRobo-Software supplied by the manufacturer.

Modified Measurement of resection tracks (BrdU). 24 hours before fixation cells were incubated with 10 μM BrdU and then 10 μM Olaparib for the last 16 hrs of treatment. Cells were trypsinized and resuspended in ice cold PBS to a concentration of 10 x 10^5 cells/ml. In order to lyse the cells, 2 μl of sample was placed on a slide and mixed with 7 μl of spreading buffer (200 mM Tris pH 7.4, 50 mM EDTA, 0.5% SDS) and incubated for 2 mins. Slides were then placed at a shallow angle to cause the droplet to gradually run down the slide, ensuring constant movement of the droplet. Slides were then fixed in 3:1 MeOH: AcOH for 10 mins and then stored at 4°C.

Slides were washed in PBS and Blocking solution (2g BSA, 200 μl Tween 20, 200 ml PBS) and then incubated with mouse anti BrdU primary antibody. Slides were then incubated with AlexaFluor Rabbit anti mouse 488. Images were taken on the Leica DM6000B microscope and analysis performed using ImageJ software. Lengths were calculated using a scale bar to convert pixels to μm and this ratio, of 3.493 pixels per μm, was used to measure BrdU track lengths. 50 fibers per treatment were measured and plotted on a Whisker plot using Graphpad.

Immunoprecipitation. BARD1-Flp-In^{TM} 293 cells were Doxycyclin (1μg/ml) treated for 48 hours and lysed in cold Nuclear Lysis Buffer (10 mM HEPES pH7.6, 200 mM sodium chloride, 1.5 mM magnesium chloride, 10% glycerol, 0.2 mM EDTA, 1% Triton). For every 10 ml of nuclear lysis buffer, 1 Complete protease inhibitor tablet, 1 PhosSTOP phosphatase inhibitor tablet (Roche), and 1 μl DNase were added. Pre-cleared lysate combined with washed Flag-agarose beads (Sigma) was incubated with rotation overnight at 4°C. After 3 x 1 ml PBS-0.02% Tween washes, all wash buffer was removed before either adding 2 x loading buffer, boiled and loaded onto an SDS PAGE gel and analyzed by western blotting or used for an E3 ligase assay.

Nickel-precipitations. (Enrichment of Ubiquitin-conjugates). Cells transfected with Hisx6-myc-Ubiquitin were lysed directly in 8 M urea buffer (8 M Urea, 0.1 M sodium phosphate pH6.3, 0.01 M Tris–HCl pH 6.3, 10 mM β-mercaptoethanol, 5 mM imidazole plus 0.2% Triton-X-100) harvested and sonicated. They were then mixed with His-Select beads (Sigma) and incubated overnight at 4 °C, washed and eluted in sample loading buffer.

Immunofluorescence. Cells were plated on 13 mm circular glass coverslips at a density of 5 x 10^4 cells/ml, treated as required. For RPA, BLM and RAD51 staining cells were pre-extracted in CSK buffer (100 mM sodium chloride, 300 mM sucrose, 3 magnesium chloride, 10 mM PIPES pH 6.8) for 1 minute at room temperature, For all other staining cells were first fixed in 4% PFA and permeabilized with 0.2% TritonX100 in PBS. After blocking in 10% FCS, cells were incubated with primary antibody for 1 hr (unless otherwise stated) and with secondary AlexaFluor antibodies for 1 hour. The DNA was stained using Hoechst at 1:20,000. In some images the DNA stain has been drawn around (but not shown) to illustrate the location of the

nucleus.

EdU staining. Cells were incubated with the nucleoside analogue EdU (5-ethynyl-2'-deoxyuridine) at 10 μM final concentration for 2 hours (RAD51/RPA experiments) or 1 hour super-resolution imaging prior to fixation. Staining was carried it out following Click-iT® EdU Imaging Kits (Life Technologies) according to the manufacturer.

Microscopy. For RPA stains: Images of immunofluorescent staining were captured on the Zeiss 510 Meta confocal microscope, using three lasers to give excitation at 647, 555 and 488 nM wavelengths. Images at each wavelength were collected sequentially at a resolution of approximately 1024 x 1024 pixels, using the Plan-Apochromat 100x/1.4 Oil objective. All other immunofluorescent staining was imaged using the Leica DM6000B microscope using a HBO lamp with 100W mercury short arc UV bulb light source and four filter cubes, A4, L5, N3 and Y5 to produce excitations at wavelengths 360 488, 555 and 647 nm respectively. Images were captured at each wavelength sequentially using the Plan Apochromat HCX 100x/1.4 Oil objective at a resolution of 1392x1040 pixels.

High-resolution fluorescence microscopy. Z-stack images were taken on an Olympus DeltaVision IX70 microscope. Using softWoRx imaging software, z-stacks were taken over 2μm at 0.1μm intervals at 100x magnification. The images were then deconvolved using softWoRx deconvolution software. Fluorescence intensity profiles were also generated using softWoRx to analyse 30 foci profiles per experiment.

Statistics. Statistical analysis was by two-sided Students T-test throughout. *<p0.05, **p<0.01, ***P<0.005. All center values are given as the mean and all error bars are standard error about the mean (s.e).

References to Online Methods

44. Boutell, C., Sadis, S. & Everett, R.D. Herpes simplex virus type 1 immediate-early protein ICP0 and is isolated RING finger domain act as ubiquitin E3 ligases in vitro. *J Virol* **76**, 841-50 (2002).

45. Lukas, C., Falck, J., Bartkova, J., Bartek, J. & Lukas, J. Distinct spatiotemporal dynamics of mammalian checkpoint regulators induced by DNA damage. *Nat Cell Biol* **5**, 255-60 (2003).

Figure 1

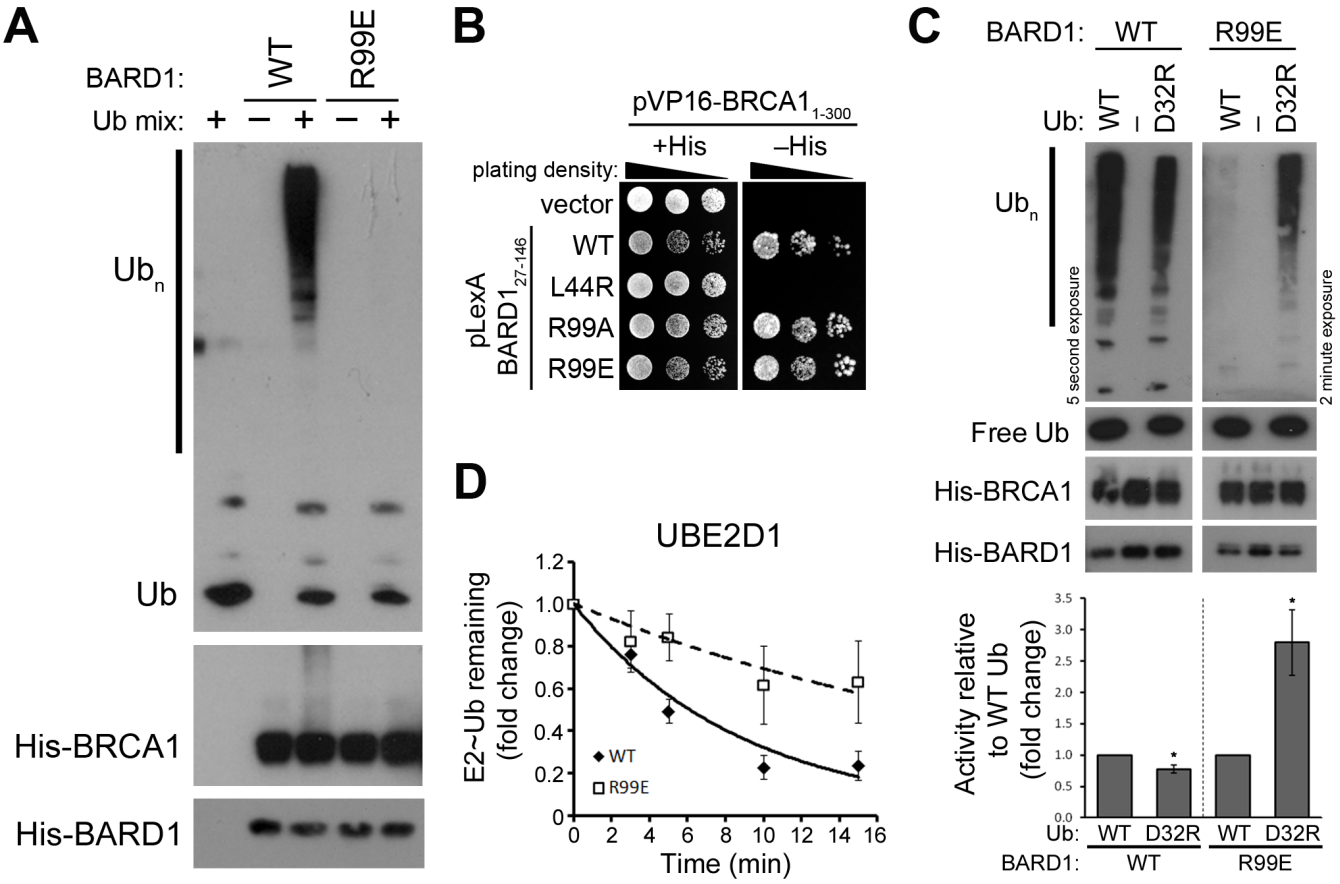
A
BARD1:
WT
R99E
Ub mix: + – + – +
Ub$_n$
Ub
His-BRCA1
His-BARD1
B
pVP16-BRCA1$_{1-300}$
+His
–His
plating density:
vector
WT
L44R
R99A
R99E
pLexA BARD1$_{27-146}$
C
BARD1: WT R99E
Ub: WT – D32R WT – D32R
Ub$_n$
5 second exposure
2 minute exposure
Free Ub
His-BRCA1
His-BARD1
Activity relative to WT Ub (fold change)
Ub: WT D32R WT D32R
BARD1: WT R99E
D
UBE2D1
E2~Ub remaining (fold change)
WT
R99E
Time (min)

Figure 2

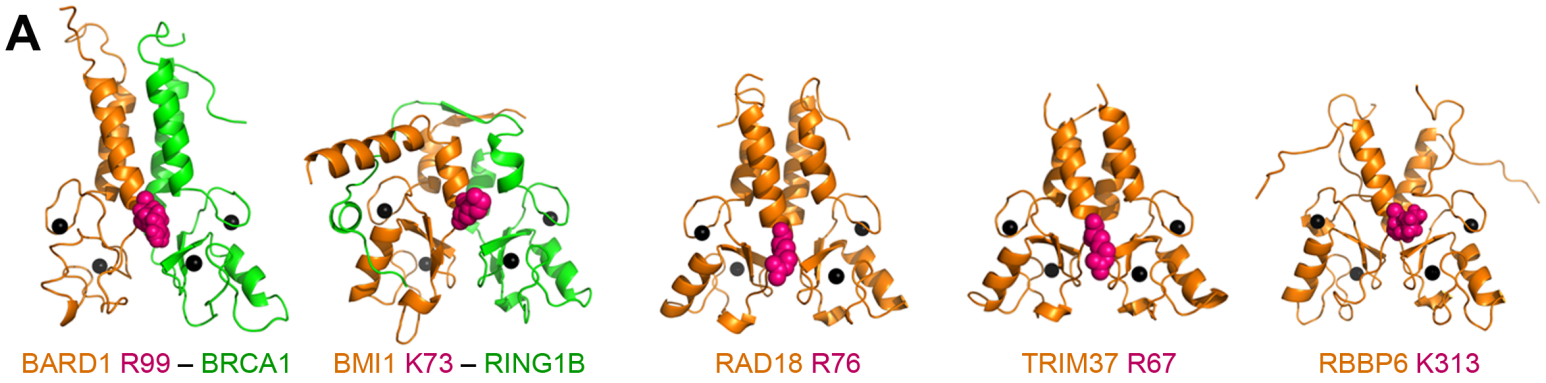
A
BARD1 R99 – BRCA1
BMI1 K73 – RING1B
RAD18 R76
TRIM37 R67
RBBP6 K313
B
+ UV
HA-RAD18: – WT R76A – WT R76A
PCNA
long
short
PCNA-Ub
PCNA
HA-RAD18
β-actin
C
BMI1: WT K73E
RING1B/BMI1:
Ub mix: + – + – + – + – + – + –
H2A
H2A-Ub
H2A
BMI1

Figure 3

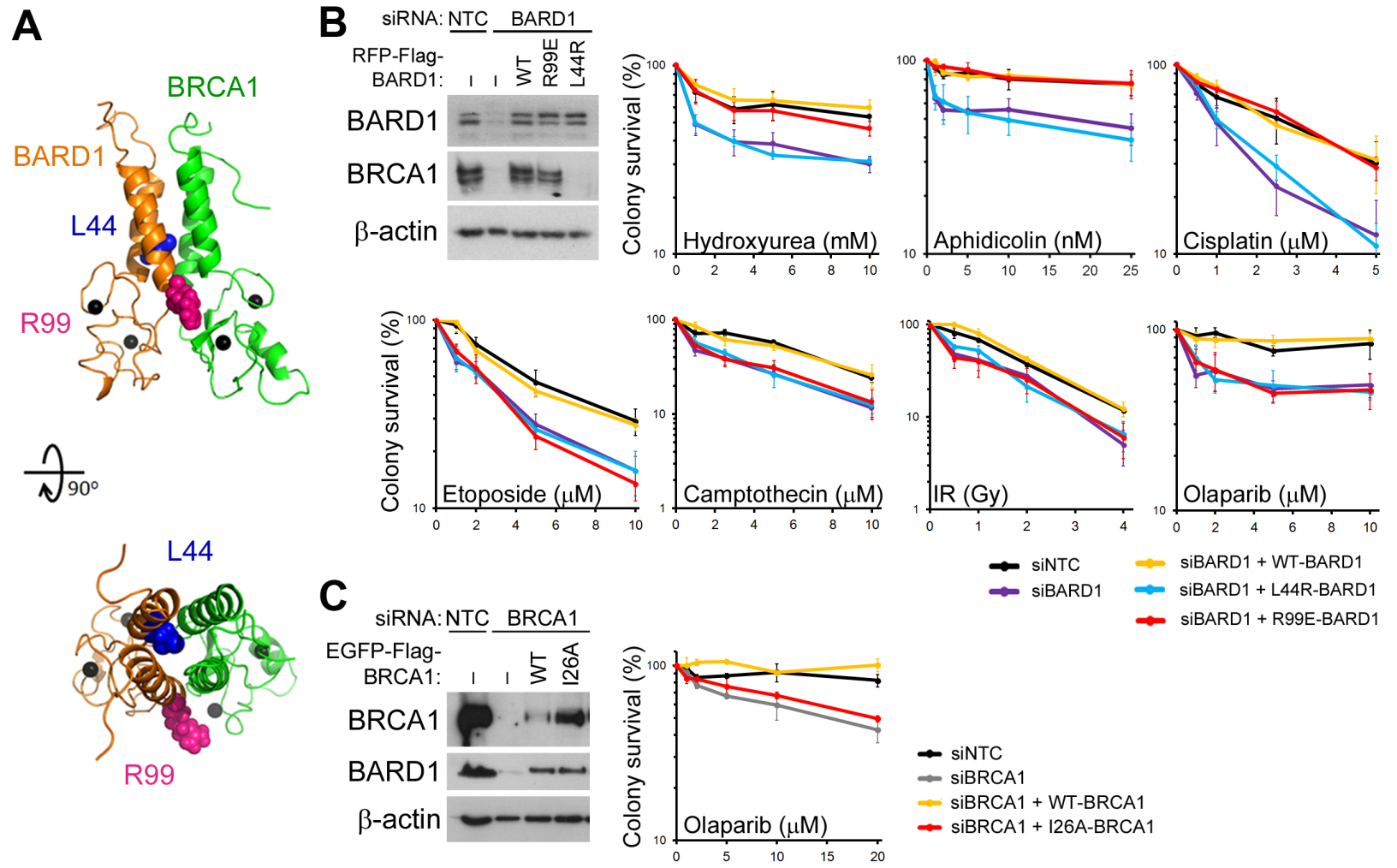
A
BRCA1
BARD1
L44
R99
90°
L44
R99
B
siRNA: NTC BARD1
RFP-Flag-BARD1: - - WT R99E L44R
BARD1
BRCA1
β-actin
Colony survival (%)
Hydroxyurea (mM)
Aphidicolin (nM)
Cisplatin (μM)
Etoposide (μM)
Camptothecin (μM)
IR (Gy)
Olaparib (μM)
siNTC
siBARD1
siBARD1 + WT-BARD1
siBARD1 + L44R-BARD1
siBARD1 + R99E-BARD1
C
siRNA: NTC BRCA1
EGFP-Flag-BRCA1: - - WT I26A
BRCA1
BARD1
β-actin
Colony survival (%)
Olaparib (μM)
siNTC
siBRCA1
siBRCA1 + WT-BRCA1
siBRCA1 + I26A-BRCA1

Figure 4

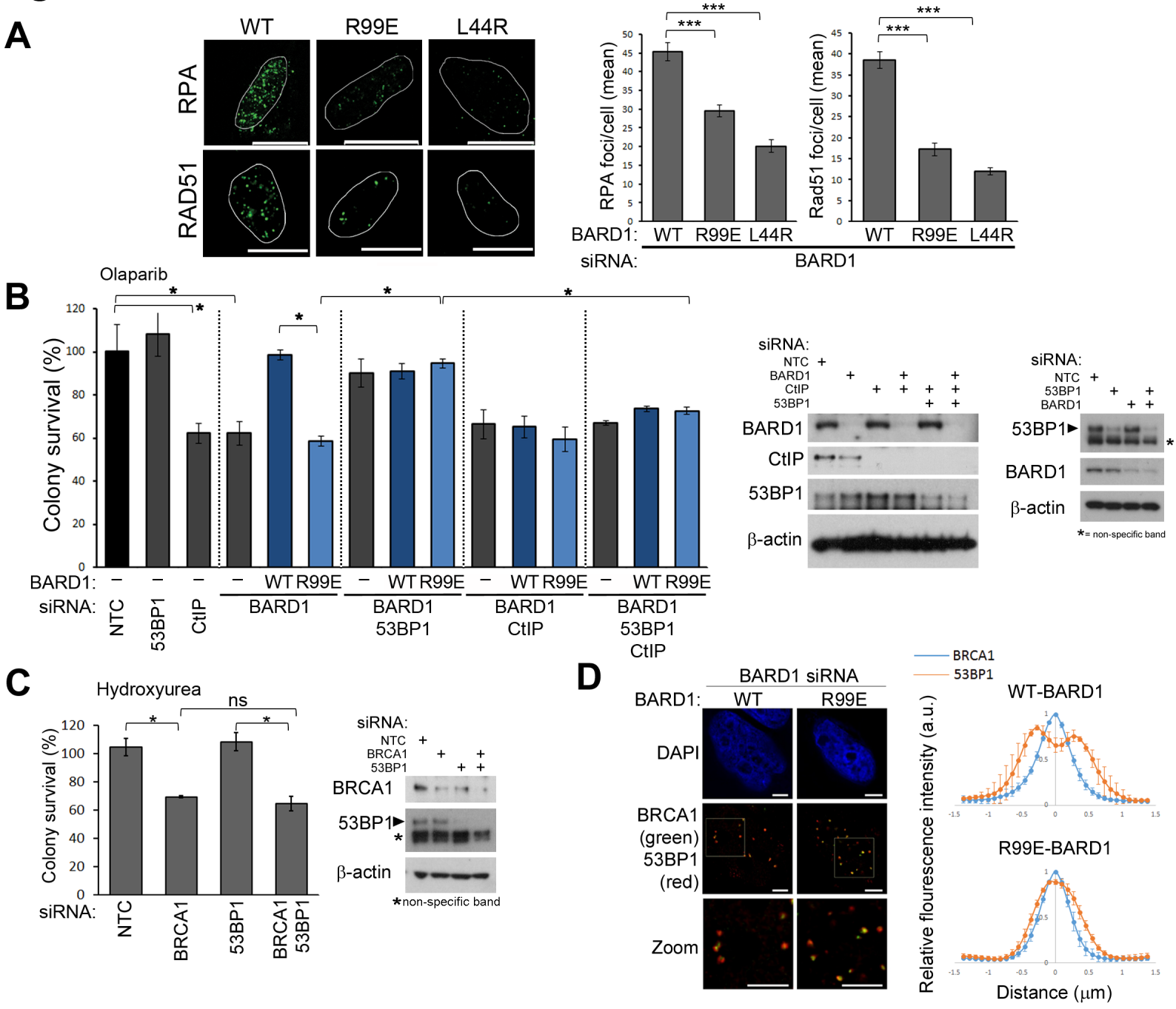
A
WT
R99E
L44R
RPA
RAD51
RPA foci/cell (mean)
Rad51 foci/cell (mean)
***
BARD1: WT R99E L44R
siRNA: BARD1
B
Olaparib
Colony survival (%)
BARD1: – – – – WT R99E – WT R99E – WT R99E – WT R99E
siRNA: NTC 53BP1 CtIP BARD1 BARD1 53BP1 BARD1 CtIP BARD1 53BP1 CtIP
siRNA:
NTC
BARD1
CtIP
53BP1
BARD1
CtIP
53BP1
β-actin
53BP1
BARD1
β-actin
*= non-specific band
C
Hydroxyurea
ns
Colony survival (%)
siRNA: NTC BRCA1 53BP1 BRCA1 53BP1
BRCA1
53BP1
β-actin
*non-specific band
D
BARD1 siRNA
BARD1: WT R99E
DAPI
BRCA1 (green) 53BP1 (red)
Zoom
BRCA1
53BP1
WT-BARD1
R99E-BARD1
Relative flourescence intensity (a.u.)
Distance (μm)

Figure 5

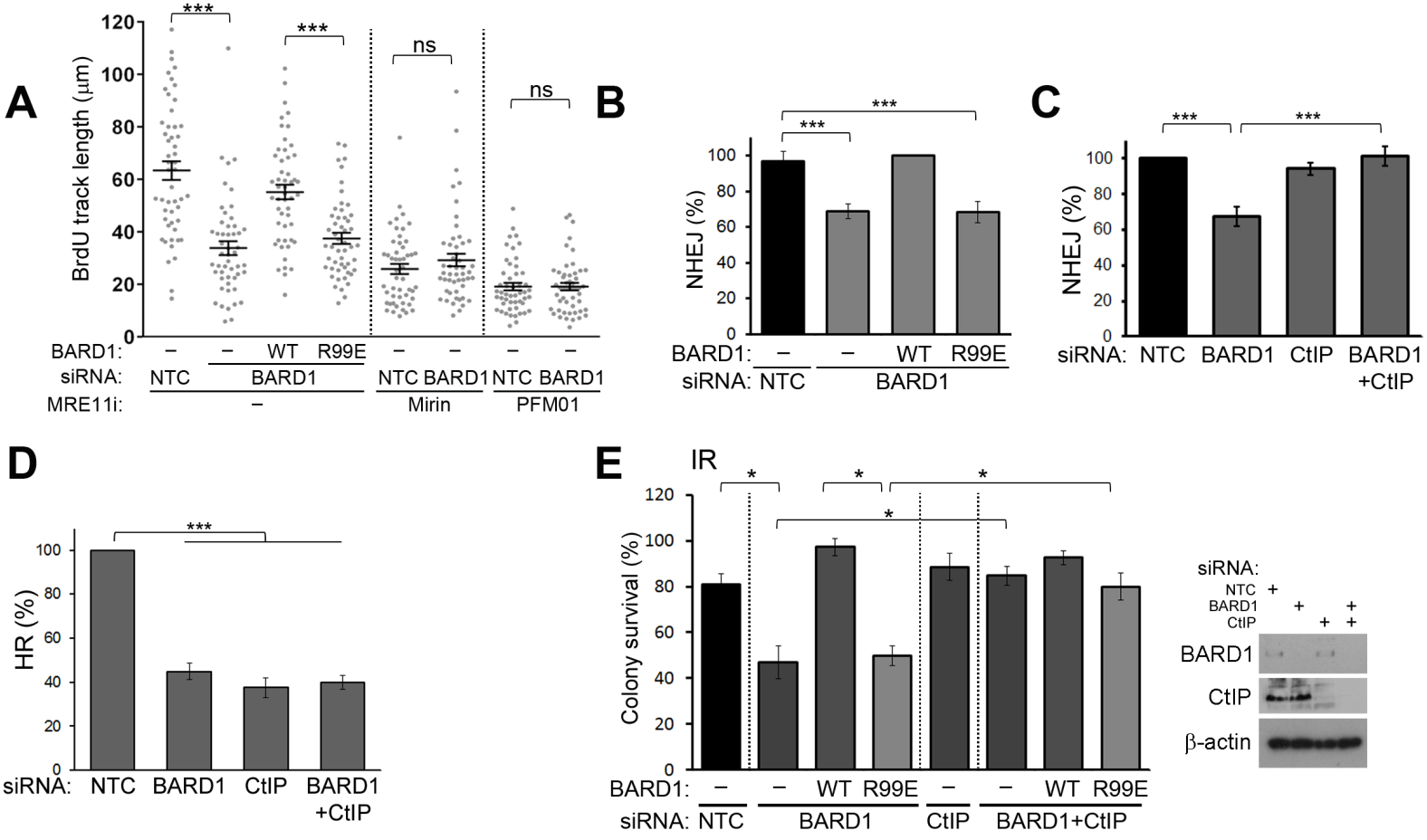
A
BrdU track length (μm)
***
***
ns
ns
BARD1: – – WT R99E – – – –
siRNA: NTC BARD1 NTC BARD1 NTC BARD1
MRE11i: – Mirin PFM01
B
NHEJ (%)
***
***
BARD1: – – WT R99E
siRNA: NTC BARD1
C
NHEJ (%)
***
***
siRNA: NTC BARD1 CtIP BARD1 +CtIP
D
HR (%)
***
siRNA: NTC BARD1 CtIP BARD1 +CtIP
E
IR
Colony survival (%)
BARD1: – – WT R99E – – WT R99E
siRNA: NTC BARD1 CtIP BARD1+CtIP
siRNA:
NTC +
BARD1 + +
CtIP + +
BARD1
CtIP
β-actin

Figure 6

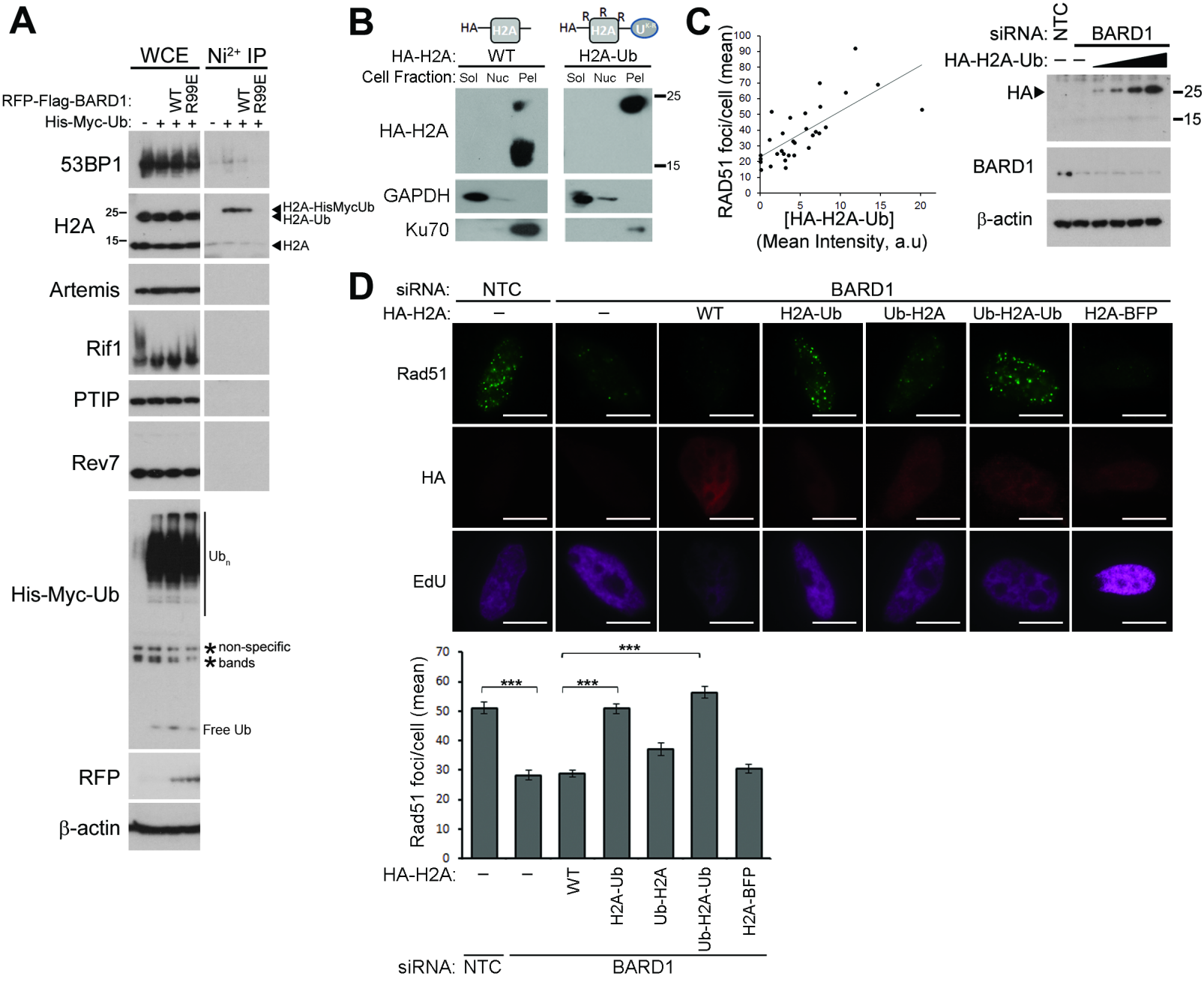
A
WCE
Ni2+ IP
RFP-Flag-BARD1:
WT
R99E
His-Myc-Ub:
53BP1
H2A
25
15
H2A-HisMycUb
H2A-Ub
H2A
Artemis
Rif1
PTIP
Rev7
His-Myc-Ub
Ubn
non-specific bands
Free Ub
RFP
β-actin
B
HA
H2A
Ub
HA-H2A:
WT
H2A-Ub
Cell Fraction:
Sol Nuc Pel
HA-H2A
GAPDH
Ku70
25
15
C
RAD51 foci/cell (mean)
[HA-H2A-Ub]
(Mean Intensity, a.u)
siRNA:
NTC
BARD1
HA-H2A-Ub:
HA
BARD1
β-actin
25
15
D
siRNA:
NTC
BARD1
HA-H2A:
–
WT
H2A-Ub
Ub-H2A
Ub-H2A-Ub
H2A-BFP
Rad51
HA
EdU
Rad51 foci/cell (mean)
***
***
***
HA-H2A:
–
–
WT
H2A-Ub
Ub-H2A
Ub-H2A-Ub
H2A-BFP
siRNA:
NTC
BARD1

Figure 7

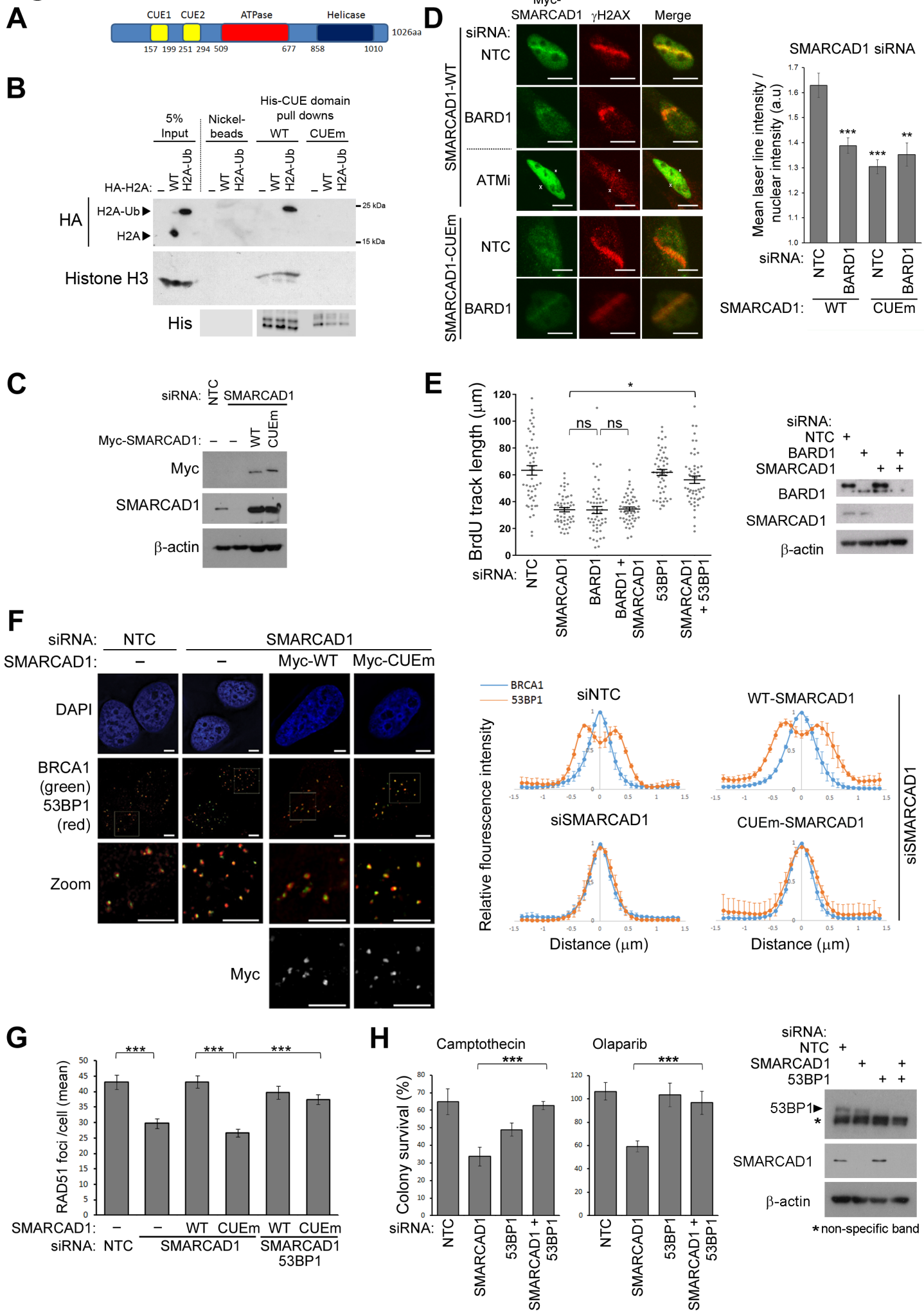
A
CUE1
CUE2
ATPase
Helicase
1026aa
157 199 251 294 509 677 858 1010
B
5% Input
Nickel-beads
His-CUE domain pull downs
WT
CUEm
HA-H2A:
WT H2A-Ub
HA
H2A-Ub
H2A
25 kDa
15 kDa
Histone H3
His
C
siRNA: NTC SMARCAD1
Myc-SMARCAD1: – – WT CUEm
Myc
SMARCAD1
β-actin
D
Myc-SMARCAD1
γH2AX
Merge
siRNA:
NTC
BARD1
ATMi
SMARCAD1-WT
SMARCAD1-CUEm
SMARCAD1 siRNA
Mean laser line intensity / nuclear intensity (a.u)
***
**
siRNA: NTC BARD1 NTC BARD1
SMARCAD1: WT CUEm
E
BrdU track length (μm)
ns
*
siRNA: NTC SMARCAD1 BARD1 BARD1 + SMARCAD1 53BP1 SMARCAD1 + 53BP1
siRNA: NTC + BARD1 + + SMARCAD1 + +
BARD1
SMARCAD1
β-actin
F
siRNA: NTC SMARCAD1
SMARCAD1: – – Myc-WT Myc-CUEm
DAPI
BRCA1 (green) 53BP1 (red)
Zoom
Myc
BRCA1
53BP1
siNTC
WT-SMARCAD1
siSMARCAD1
CUEm-SMARCAD1
Relative flourescence intensity
Distance (μm)
siSMARCAD1
G
RAD51 foci /cell (mean)
***
SMARCAD1: – – WT CUEm WT CUEm
siRNA: NTC SMARCAD1 SMARCAD1 53BP1
H
Camptothecin
Olaparib
Colony survival (%)
siRNA: NTC SMARCAD1 53BP1 SMARCAD1 + 53BP1
siRNA: NTC + SMARCAD1 + + 53BP1 + +
53BP1
*
SMARCAD1
β-actin
* non-specific band

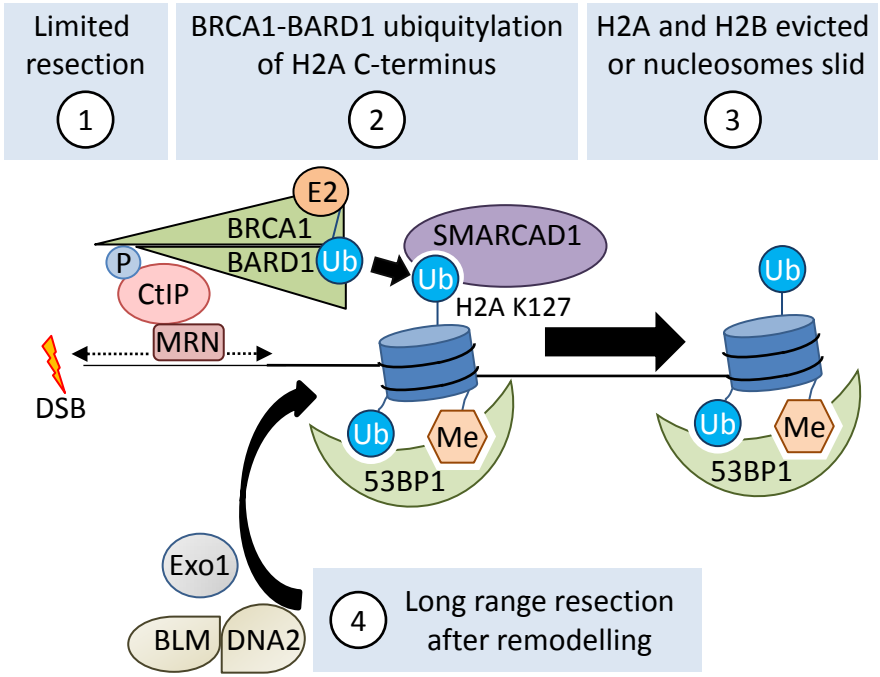
Limited resection
1
BRCA1-BARD1 ubiquitylation of H2A C-terminus
2
H2A and H2B evicted or nucleosomes slid
3
E2
BRCA1
BARD1
Ub
P
CtIP
MRN
DSB
SMARCAD1
Ub
H2A K127
Ub
Me
53BP1
Ub
Me
53BP1
Exo1
BLM
DNA2
4
Long range resection after remodelling